Title:
Genome editing reveals a role for OCT4 in human embryogenesis

Authors:
Norah M.E. Fogarty[1], Afshan McCarthy[1], Kirsten E. Snijders[2], Benjamin E. Powell[3], Nada Kubikova[4], Paul Blakeley[1], Rebecca Lea[1], Kay Elder[5], Sissy E. Wamaitha[1], Daesik Kim[6], Valdone Maciulyte[3], Jens Kleinjung[7], Jin-Soo Kim[5,7], Dagan Wells[4], Ludovic Vallier[2,9], Alessandro Bertero[2,10], James M.A. Turner[3], Kathy K. Niakan[1*]

Affiliations:
1. Human Embryo and Stem Cell Laboratory, The Francis Crick Institute, 1 Midland Road, London, NW1 1AT, UK.

2. Wellcome Trust and MRC Cambridge Stem Cell Institute and Biomedical Research Centre, Anne McLaren Laboratory, Department of Surgery, University of Cambridge, CB2 0SZ, UK

3. Sex Chromosome Biology Laboratory, The Francis Crick Institute, London, NW1 1AT, UK.

4. University of Oxford, Nuffield Department of Obstetrics and Gynaecology, John Radcliffe Hospital, Oxford OX3 9DU, UK.

5. Bourn Hall Clinic, Bourn, Cambridge CB23 2TN, UK.

6. Department of Chemistry, Seoul National University, Seoul, 151-747, Republic of Korea.

7. Bioinformatics Facility, The Francis Crick Institute, 1 Midland Road, London, NW1 1AT, UK.

8. Center for Genome Engineering, Institute for Basic Science, Daejeon, 34047, Republic of Korea.

9. Wellcome Trust Sanger Institute, Wellcome Genome Campus, Hinxton, Cambridge, CB10 1SA, UK.

10. Present address: Department of Pathology, University of Washington, Seattle, WA 98109, USA.

*Corresponding author: kathy.niakan@crick.ac.uk

Summary:
During early human development, the totipotent zygote differentiates into a blastocyst comprised of pluripotent epiblast cells, which form the fetus, and extra-embryonic cells that contribute to the placenta and yolk sac. Despite their fundamental biological and clinical importance, the molecular mechanisms that regulate these first cell fate decisions are unclear. Here we use CRISPR/Cas9-mediated genome editing to investigate the function of the pluripotency transcription factor OCT4 during human embryogenesis. Using an inducible human embryonic stem cell (hESC)-based system we identified the most efficient OCT4-targeting single guide RNA (sgRNA). By testing homologous sgRNAs in mouse zygotes we further validated sgRNAs *in vivo* and optimised microinjection techniques. Using these refined methods, we then efficiently and specifically targeted *OCT4* in diploid human zygotes

and observed compromised blastocyst development. Transcriptomics analysis revealed that *OCT4*-null cells downregulated the expression of not only extra-embryonic trophectoderm genes, such as *CDX2* and *HAND1*, but also regulators of the pluripotent epiblast, including *NANOG*. By contrast mouse embryos maintained the expression of orthologous genes, and blastocyst development is established, but maintenance is compromised. Altogether, we conclude that CRISPR/Cas9-mediated genome editing is a powerful method to interrogate gene function in the context of human development.

Introduction

Early mammalian embryogenesis is controlled by mechanisms governing the balance between pluripotency and differentiation. Expression of early lineage-specific genes varies significantly between species[1-3] with implications for developmental control and stem cell derivation. However, the mechanisms patterning the human embryo are unclear, because methods to efficiently perturb gene expression of early lineage specifiers in this species have been lacking.

The efficiency of genetic modification has significantly increased due to recent advances in genome editing using the CRISPR (clustered regularly interspaced, short palindromic repeat)/Cas (CRISPR-associated) system. The *Streptococcus pyogenes* Cas9 endonuclease is guided to homologous DNA sequences via a single-guide RNA (sgRNA) whereby it induces double strand breaks (DSBs) at the target site[4]. Several endogenous DNA repair mechanisms function to resolve the DSBs, including error-prone non-homologous or micro-homology mediated end joining, which can lead to insertions or deletions (indels) of nucleotides that can result in the null mutation of the target gene. CRISPR/Cas9-mediated editing has been attempted in abnormally fertilised tripronuclear and a limited number of normally fertilised human zygotes with variable success[5-8]. To determine if CRISPR/Cas9 can be used to understand gene function in human preimplantation development, we chose to target *POU5F1*, a gene encoding the developmental regulator OCT4, as a proof-of-principle. Zygotic *POU5F1* is thought to be first transcribed between the 4- to 8-cell stage and OCT4 protein is not detectable prior to embryo genome activation (EGA) at approximately the 8-cell stage[2,3]. OCT4 perturbation would be predicted to cause a clear developmental phenotype based on studies in the mouse[9,10] and human embryonic stem cells (hESCs)[11].

By employing an inducible hESC-based system and optimising mouse zygote microinjection techniques, we identified conditions to efficiently and precisely target *POU5F1*. Live embryo imaging revealed that while OCT4-targeted human embryos initiate blastocyst formation, the inner cell mass (ICM) forms poorly, and embryos subsequently collapse. We demonstrated that OCT4 has an earlier role in the progression of the human blastocyst and that mutations affecting *POU5F1* are correlated with the downregulation of genes associated with all three preimplantation lineages, including *NANOG* (epiblast), *GATA2* (trophectoderm) and *GATA4* (primitive endoderm). By contrast, in OCT4-null mouse blastocysts, genes such as *Nanog* continue to be expressed in the inner cell mass. The insights gained from these investigations advance our understanding of human development and suggest that there may be distinct mechanisms of lineage specification between these species.

Results

Selection of a highly-efficient sgRNA targeting *POU5F1* in hESCs

To target *POU5F1*, we selected 4 sgRNAs using a standard *in silico* prediction tool[12]: two targeting the exon encoding the N-terminal domain of OCT4 (sgRNA1-1 and sgRNA1-2), one targeting the exon encoding the conserved DNA binding POU homeodomain[13,14] (sgRNA2b) and one targeting the end of the POU domain and start of the C-terminal domain (sgRNA4)

(Extended Data Fig. 1a). To screen candidate sgRNAs we took advantage of hESCs as an unlimited resource that reflects the cellular context of the human preimplantation embryo. We engineered isogenic hESCs constitutively expressing the Cas9 gene, together with a tetracycline-inducible sgRNA[11] (Fig. 1a), thereby allowing for comparative assessment of sgRNA activities.

Cells were collected every day for 5 days for flow cytometry analysis, which revealed that induction of each of the sgRNAs in hESCs imposed remarkably different temporal effects on OCT4 protein expression (Extended Data Fig. 1b). sgRNA2b was most efficient at rapidly causing loss of OCT4 protein expression, with only 15.6% of cells retaining detectable OCT4 by day 5 (d5) of induction. Immunofluorescence analysis following sgRNA2b induction confirmed the efficient knockdown of OCT4 expression (Fig. 1b, Extended Data Fig. 2a). Conversely, in hESCs induced to express sgRNAs 1-1, 1-2, or 4, 70.5%, 43.7% and 51.7% of cells retained OCT4 expression at the equivalent time-point, respectively (Extended Data Fig. 1b). To determine the transcriptional consequences of OCT4 depletion, we performed qRT-PCR and RNA-sequencing (RNA-seq) analysis on induced and non-induced sgRNA2b-expressing hESCs (Extended Data Figs. 1c,d and 2b). sgRNA2b-induction resulted in downregulation of pluripotency genes such as *NANOG*, *ETS1* and *DPPA3* consistent with OCT4 depletion causing exit from self-renewal. Furthermore, *PAX6*, *SOX17*, *SIX3*, *GATA2* and *SOX9* were upregulated following sgRNA2b-induction, suggesting that OCT4 normally restrains differentiation (Extended Data Figs. 1c,d, Extended Data Fig. 2a,b).

Stereotypic *POU5F1* on-target indel mutations and targeting specificity in hESCs

To compare the on-target editing efficiencies and mutation spectrums induced by candidate sgRNAs, we performed a time-course genotypic analysis on cells collected across 4 days following sgRNA induction. Targeted deep sequencing of the on-target site revealed indels from as early as 24 h post-induction of sgRNA2b, but not until 48 h post-induction of sgRNAs1-1, 1-2 or 4 (Fig. 1c). sgRNA2b-induced indels most commonly comprised a 2 bp deletion upstream of the PAM site leading to a frameshift mutation and a premature stop codon (Extended Data Fig. 3), consistent with the loss of OCT4 protein expression.

We evaluated putative off-target sites identified by their sequence similarity to the seed region of sgRNA2b (Extended Data Fig. 4a,b). We did not observe off-target indels in sgRNA2b-induced hESCs, nor any sequence alterations above background PCR error rates observed in control hESC lines. In parallel we performed a genome-wide unbiased evaluation of off-target events using Digenome-seq (Extended Data Fig. 4c). Targeted deep sequencing across the experimentally determined putative off-target sites revealed that indels had only occurred at the on-target site (Extended Data Fig. 4d). Furthermore, we used the WebLogo program to determine the most frequent sequences associated with putative sites identified from Digenome-seq[15,16] (Extended Data Fig. 4e). Deep sequencing at these sites also confirmed that no off-target events had occurred (Extended Data Fig. 4f). In all, due to both its efficient mutagenicity and high on-target specificity, sgRNA2b appeared most promising.

sgRNA activity during mouse preimplantation development

We used published sgRNA/Cas9 mRNA zygote microinjection conditions[17] to further assess sgRNA activity and optimize microinjection methodologies in mouse zygotes. As it has been shown that OCT4-null mouse blastocysts lack expression of the primitive endoderm marker SOX17 due to a cell-autonomous requirement for FGF4/MAPK signaling[9,18], we used absence of both OCT4 and SOX17 immunostaining to identify OCT4-deficient embryos (Fig. 1d). This OCT4-null phenotype was observed in 54% of embryos injected with Cas9 mRNA and sgRNA2b, and in 0%, 10% or 3% of embryos injected with sgRNA1-1, sgRNA1-2 or sgRNA4, respectively (Fig. 1e). These data confirm that sgRNA2b is superior to other tested

sgRNAs at inducing null mutations in both mouse embryos and hESCs. We next interrogated a greater range of Cas9 mRNA and sgRNA concentrations to identify conditions that may enhance rates of mutagenesis (Extended Data Fig. 5a). We confirmed that the previously reported concentration of 100 ng/μl Cas9 mRNA together with 50 ng/μL sgRNA[17] is optimal for inducing an OCT4-null phenotype.

It has been suggested that microinjection of sgRNA/Cas9 ribonucleoprotein complexes may reduce mosaicism and allelic complexity by bypassing the requirement for Cas9 translation and sgRNA/Cas9 complex formation in embryos[19,20]. To test this, we microinjected mouse pronuclear zygotes with preassembled ribonucleoprotein complexes containing varying concentrations of Cas9 protein (20 – 200 ng/μL) and sgRNA2b (20 – 100 ng/μL; Fig. 1f and Extended Data Fig. 5b). Immunofluorescence analysis revealed that the sgRNA/Cas9 complex was superior to Cas9 mRNA in causing loss of both OCT4 and SOX17, and that the optimal concentration comprised 50 ng/μL Cas9 protein and 25 ng/μL sgRNA (Fig. 1f). Interestingly, MiSeq analysis demonstrated that 83.3% of blastocysts derived from sgRNA2b/Cas9 complex microinjections had 4 or fewer different types of indels (Fig. 1g), suggesting that editing occurred prior to, or at the 2-cell stage. By contrast, only 52.6% of sgRNA2b/Cas9 mRNA microinjected embryos exhibited this range of indels. Furthermore, a greater proportion of blastocysts formed after sgRNA2b/Cas9 mRNA microinjection had 6 or more different types of detectable indels (42.2%) compared to the sgRNA2b/Cas9 complex (8.3%). This increased mutational spectrum suggests that following Cas9 mRNA injection, DNA editing occurred between the 3- to 4-cell stage. Consistent with previous reports[21], we observed a stereotypic pattern in the type of indels detected in independently targeted embryos, including the representative 28 bp deletion (Extended Data Fig. 5c), which was distinct from those induced in hESCs.

In addition to lacking SOX17 and OCT4 expression, mouse embryos microinjected with the sgRNA2b/Cas9 complex recapitulated other reported OCT4-null phenotypes such as downregulation of PDGFRA, SOX7, GATA6 and GATA4 in the primitive endoderm (Extended Data Fig. 5d). Consistent with the role of OCT4 in repressing TE genes[9], the few inner cell mass (ICM) cells that could be detected in sgRNA2b/Cas9 microinjected embryos ectopically expressed CDX2 (Extended Data Fig. 5d). When plated in mouse ESC derivation conditions, these embryos failed to generate ICM outgrowths, and instead exhibited differentiation to trophoblast-like cells (Extended Data Fig. 5e). In contrast, blastocysts derived from non-injected embryos formed ICM outgrowths in most instances, as did blastocysts from embryos microinjected with Cas9 protein alone or an sgRNA/Cas9 complex targeting *Dmc1* (a gene not essential for preimplantation development). Having thus determined sgRNA2b to be an efficient and specific guide capable of generating a null mutation of *POU5F1*/*Pou5f1* in both hESCs and mouse preimplantation embryos, we next used this together with our optimized microinjection technique to target *POU5F1* in human preimplantation embryos.

Targeting *POU5F1* in human preimplantation embryos

To determine the requirement for OCT4 in human embryos, we performed CRISPR editing on thawed *in vitro* fertilized zygotes that were donated as surplus to infertility treatment. We microinjected 37 zygotes with the sgRNA2b/Cas9 ribonucleoprotein complex (Supplementary Video 1), and 17 zygotes with Cas9 protein alone, to control for the microinjection technique. Of the sgRNA2b/Cas9 microinjected zygotes, 30 embryos retained both pronuclei during microinjection with pronuclear fading observed approximately 6 hours later, followed by cytokinesis on average 5 hours later (Supplementary Video 2). These timings are similar to those previously published[22,23] and indicate that microinjection was performed when the embryos were in S-phase of the cell cycle (Fig. 2a). Genome editing via the ribonucleoprotein

complex has been estimated to start after approximately 3 hours *in vitro* and persist for 12-24 hours[24], therefore CRISPR/Cas9-induced DSBs are likely to be formed during late S-phase, or subsequently at G2 phase. In 7 sgRNA2b/Cas9 microinjected zygotes, the pronuclei had already faded after thawing, thus they had exited S-phase and were undergoing syngamy. These embryos consequently underwent cell division approximately 3 hours after microinjection. In these embryos editing likely occurred at the G2 or M phase, or in the G1 phase of the next cell cycle, at the 2-cell stage (Fig. 2a), which would promote mosaicism.

Time-lapse microscopy of the embryos showed that the timings of cleavage divisions following pronuclear fading were similar between the Cas9 protein and the sgRNA2b/Cas9 microinjected embryos (Fig. 2b,c). By the 8-cell stage, cleavage arrest was observed in 43% (16 out of 37) of sgRNA2b/Cas9 microinjected embryos compared to 41% (10 out of 17) Cas9 protein control embryos (Fig. 2d). As developmental arrest at the onset of EGA at the 8-cell stage strongly correlates with aneuploidy in IVF embryos[25], we also sought to determine embryo karyotype. We performed low-pass whole genome sequencing, which has been shown to accurately estimate gross chromosome anomalies[26]. We collected blastomeres from sgRNA2b/Cas9 microinjected embryos arrested up to the 8-cell stage and detected chromosomal loss or gain in 83% (5 out of 6) of embryos (Extended Data Fig. 6a), which is consistent with rates reported by preimplantation genetic screening[26,27]. Trophectoderm biopsies of a subset of blastocysts that developed following sgRNA2b/Cas9 microinjection determined that 60% (3 out of 5) were euploid (Fig. 2e, Extended Data Fig. 6a). The other two blastocysts exhibited karyotypic abnormalities including the loss of chromosome 16 (Extended Data Fig. 6b), an abnormality frequently observed in human preimplantation embryos and thus likely to be unrelated to targeting[25]. In the Cas9 protein control group, 57% (4 out of 7) of blastocysts were euploid, and aneuploidies were observed in the remaining 3 blastocysts, including the loss of chromosome 14 in two sibling-matched control embryos, and the gain of chromosome 15 and 18 (Fig. 2e, Extended Data Fig. 6a,b). Altogether, this suggests that CRISPR/Cas9 targeting does not increase the rates of karyotypic anomalies in human embryos.

47% (8 out of 17) of Cas9 protein microinjected controls developed to the blastocyst stage, a rate equivalent to those of uninjected controls[28], suggesting that the microinjection technique did not affect embryo viability (Fig. 2d). However, only 19% (7 out of 37) of sgRNA2b/Cas9 protein microinjected embryos developed to the blastocyst stage, significantly fewer compared to Cas9 protein microinjected controls (Fig. 2d, $P<0.05$). The blastocysts that formed following sgRNA2b/Cas9 protein microinjection were of variable quality (Extended Data Fig. 6c). Although all blastocysts had a discernible blastocoel cavity, only some possessed a small compact ICM (Extended Data Fig. 6c), and all retained a thick zona pelucida, in contrast to Cas9 microinjected controls. sgRNA2b/Cas9 microinjected human embryos also went through iterative cycles of expanding and initiating blastocyst formation and then collapsing until some embryos ultimately degenerated (Supplementary Video 2 and 3). Altogether, this suggests that targeting OCT4 in human embryos impacts both blastocyst viability and quality.

To determine on-target editing efficiency, we performed targeted deep and/or Sanger sequencing of all cells microdissected from the sgRNA2b/Cas9 microinjected embryos arrested prior to the 8-cell stage, and found indels at the *POU5F1* on-target site in 71% (5 out of 7) of embryos (Fig. 3a). The most frequently observed indels in sgRNA2b/Cas9 microinjected embryos were the 2 bp and 3 bp deletions that were observed in the sgRNA2b induced hESCs (Fig. 3b, Extended Data Fig. 7a,b). This finding indicates that hESCs can be used not only to screen sgRNA efficiency, but also to predict the *in vivo* mutation spectrum induced by CRISPR/Cas9-mediated genome editing. We also detected larger *POU5F1*

deletions in the human embryos compared to hESCs, similar to our observations in mouse embryos (Fig. 3b, Extended Data Fig. 7a,b). Furthermore, targeted deep and/or Sanger sequencing in edited cells demonstrated that off-target mutations were undetectable above background PCR error rates, further confirming the specificity of the sgRNA (Extended Data Fig. 7c,d).

We next assessed mutational signatures in more developmentally advanced embryos, after EGA. Interestingly, we confirmed that on-target editing had occurred in 8 out of 8 sgRNA2b/Cas9 microinjected embryos analysed from the 8-cell to the blastocyst stage. However, invariably these embryos all retained wild-type copies of the *POU5F1* allele in at least one cell (Fig. 3a). In sgRNA2b/Cas9 microinjected human embryos, OCT4 protein expression was downregulated in most cleavage-stage cells and undetectable above background in others, confirming high efficiency of editing (Fig. 3c; Extended Data Fig. 8a). However, we were able to identify at least one cell that had nuclear OCT4 staining above background levels (Fig. 3c; Extended Data Fig. 8a). Moreover, despite a significant reduction in cell number, blastocyst-stage embryos also retained OCT4 expression in a subset of cells (Fig. 3d,e Extended Data Fig. 8b,c). These findings suggest that *POU5F1* targeting efficiency is high, and that only embryos with partial OCT4 expression are able to progress to the blastocyst stage.

To determine if there is a high degree of editing in embryos prior to the onset of OCT4 expression, we microinjected 4 additional human embryos with the sgRNA2b/Cas9 complex and stopped their development prior to the 8-cell stage. 100% (4 out of 4) of these embryos had detectable indels, with two embryos lacking wild-type *POU5F1* alleles (Fig. 3a). In one embryo editing occurred in all blastomeres, although one blastomere retained one copy of the wild-type allele. In another embryo, while 4 out of 5 blastomeres had been edited, one blastomere retained both copies of the wild-type allele. Together with the cleavage arrested embryos above, this demonstrates that in 45% (5 out of 11) of cleavage stage embryos (either stopped or developmentally arrested), all of the cells analysed from each embryo had no detectable *POU5F1* wild-type alleles, indicating high rates of editing. Altogether these data suggest an unexpectedly earlier function for OCT4 in humans compared to mice, prior to blastocyst formation.

Loss of OCT4 in human embryos is associated with mis-expression of genes associated with the three lineages in the blastocyst

To determine globally which genes might be affected by the loss of OCT4, we microdissected single cells from microinjected embryos at the blastocyst stage. We adapted a method to isolate both RNA and DNA from single cells[29] in order to perform RNA-seq and targeted deep or Sanger sequencing of on-target and putative off-target sites. Principal component analysis showed that cells from sgRNA2b/Cas9 microinjected human blastocysts clustered distinctly from those derived from Cas9 protein microinjected controls (Fig. 4a). Intriguingly, the cluster from sgRNA2b/Cas9 microinjected embryos contained not only cells that were genotypically knockout for *POU5F1*, but also those that were wild-type or heterozygous for *POU5F1*. This finding suggests that loss of *POU5F1* may impose non-cell autonomous effects on gene expression in neighbouring wild-type or heterozygous cells.

Differential gene expression analysis indicated that genes most highly mis-expressed in the sgRNA2b/Cas9 targeted human blastocysts compared to the Cas9 protein controls included those that we previously identified as highly enriched in the epiblast, including *NANOG*, *KLF17*, *DPPA5*, *ETV4*, *TDGF1*, and *VENTX* (Extended Data Fig. 9a, Supplementary Table 1). Immunofluorescence analysis confirmed that even in cells retaining OCT4, the expression of NANOG was absent (Fig. 4b, Extended Data Fig. 8c). In striking contrast, OCT4-null

mouse blastocysts maintained Nanog expression in the ICM (Fig. 4b, Extended Data Fig. 8d,e), as previously reported[9,18].

In OCT4-null cells several trophectoderm-associated genes were also significantly downregulated, including *CDX2*, *HAND1*, *DLX3*, *TEAD3*, *PLAC8* and *GATA2* (Extended Data Fig. 9a, Supplementary Table 1). We confirmed loss of GATA2 protein expression in human sgRNA2b/Cas9 protein injected embryos (Fig. 4c, Extended Data Fig. 8f). Coupled with the failure to maintain a fully expanded blastocyst, this finding suggests that the integrity of the trophectoderm may be compromised in OCT4-targeted embryos. To further characterize this, we performed immunofluorescence analysis for ZO-1, which incorporates into tight junctions during trophectoderm formation. In sgRNA2b/Cas9 targeted human blastocysts, ZO-1 expression was interrupted, patchy and diffuse compared to the uniform network-like distribution in uninjected control embryos (Fig. 4d). This is in contrast to mouse OCT4-null embryos, where expression of trophectoderm markers such as *Cdx2*, *Hand1* and *Gata3* are upregulated[9].

Additionally, primitive endoderm markers such as *GATA4* were downregulated in sgRNA2b/Cas9 microinjected embryos compared to Cas9 protein controls. Immunofluorescence analysis suggested that SOX17 protein expression was also downregulated (Fig. 3d, Extended Data Fig. 8b). Moreover, we were surprised to observe ectopic expression of *PAX6* in some cells from sgRNA2b/Cas9 edited human blastocysts (Extended Data Fig. 9a, Supplementary Table 1). The lack of expression of genes associated with all three lineages in the blastocyst suggests that OCT4-targeted embryos either failed to initiate the expression of these genes or downregulated their expression as development progressed. To determine whether the gene expression patterns in OCT4-targeted cells more closely resemble cells from earlier stages of human development, we integrated our data with a previously published dataset comprising all stages of human preimplantation development[3,30] (Fig. 4e, Extended Data Fig. 9b). This revealed that while cells from OCT4-targeted embryo were progressing towards the transcriptional state of the blastocyst, they were more dispersed and heterogeneous in their gene expression. Altogether, our data suggests that the integrity of the human blastocyst is compromised as a consequence of OCT4 downregulation. As a result, all lineages are negatively affected, pointing to a functional role for OCT4 in early human development.

Discussion

CRISPR/Cas9-mediated genome editing represents a transformative method to evaluate the function of putative regulators of human preimplantation development. We demonstrate the importance of initially screening sgRNA efficiencies and mutagenic patterns prior to targeting in human embryos, as sgRNAs were not equivalently efficient in inducing *POU5F1*-null mutations despite scoring highly by *in silico* predictions. We identify different consequences of OCT4 loss on human versus mouse embryos, consistent with other differences reported between these species. For example, pharmacological inhibition of FGF and downstream ERK signaling leads to ectopic expression of pluripotency factors in the mouse, but not the human at equivalent stages[31,32].

Surprisingly, our data suggests OCT4 may be required earlier in human development than it is in mice, for instance during the cleavage or morula stages, when OCT4 expression is initiated (Fig. 4f). As the mouse maternal/zygotic *Pou5f1*-null mutation phenocopies the zygotic-null mutation[9], it is unlikely that persistence of maternal transcripts or proteins compensates for the loss of OCT4 expression, and any additional compensatory mechanisms that may be present in the mouse do not appear to be conserved in the regulation of human development.

The mis-expression of genes associated with all three blastocyst lineages further suggests that OCT4 may have an essential function prior to this stage. In the future, it would be informative to determine whether OCT4 mutation leads to changes in gene expression prior to the blastocyst stage, which may explain the failure of blastocyst development. Alternatively, inducing *POU5F1*-null mutations in human embryos slightly later in development, following the onset of EGA, may bypass its earlier critical role and thereby delineate its function in the fully formed blastocyst.

Significantly, CRISPR/Cas9-mediated genome editing does not appear to increase genomic instability or developmental arrest prior to EGA, suggesting that this method may be used to understand the function of other putative lineage specifiers. In future, a number of adaptations may provide further advantages. Co-injection of the CRISPR/Cas9 components with sperm during intracytoplasmic sperm injection[33] may allow more time for targeting prior to the first cell division, further increasing editing efficiency. Indeed, this approach has been used recently in human embryos[8]. Introducing multiple sgRNAs may also increase targeting efficiency, but may also increase the risk of off-target mutations. Alternatively, introducing the CRISPR/Cas9 components alongside a donor oligonucleotide complementary to the target locus and harboring a premature stop codon, should favor the generation of null mutations via homology directed repair. This approach may not be straightforward given recent attempts to correct an abnormal paternal gene variant were reported to use the maternal allele for HDR rather than an introduced template[8]. Targeting genes not essential for, or with a later or more specific role in pre-implantation development will also inform our interpretation of the OCT4 phenotype. At present, we cannot be certain that the early developmental arrest is associated with the loss of OCT4 rather than some non-specific effect of injecting both Cas9 and the sgRNA, as opposed to the Cas9 alone. However, the only other study to date using genome editing with human embryos that showed development beyond 8-cell stages, where a non-essential gene was targeted, showed normal blastocyst formation at rates similar to controls[8]. This suggests that the effects we see here are due to loss of OCT4. Altogether we developed an optimized approach to target OCT4 in human embryos thus revealing a distinct function compared to the mouse. This proof of principle lays out a framework for future investigations that could transform our understanding of human biology, thereby leading to improvements in the establishment and therapeutic use of stem cells and in IVF treatments.

Acknowledgements

We would like to thank the generous donors whose contributions have enabled this research. We also thank Mike Macnamee, Phil Snell and Leila Christie for their support and assistance with the donation of embryos to this research. We thank Takayuki Hiroda and John Schimenti for providing the DMC1 sgRNA sequence and product. We thank Robin Lovell-Badge, Ian Henderson, James Haber and Janet Rossant for helpful discussions and advice. We are grateful to the Wellcome Trust policy advisers, especially Katherine Littler and Sarah Rappaport, as well as James Lawford-Davies and Melanie Chatfield for their advice and support. We would like to thank the Francis Crick Institute's Biological Resources, Advanced Light Microscopy, High Throughput Sequencing and Bioinformatics facilities. DW was supported by the National Institute for Health Research (NIHR) Oxford Biomedical Research Centre Programme. NK was supported by the University of Oxford Clarendon Fund. AB was supported by a British Heart Foundation PhD Studentship (FS/11/77/39327). LV was supported by core grant funding from the Wellcome Trust and Medical Research Council (PSAG028). J-SK was supported by the Institute for Basic Science (IBS-R021-D1). Work in the KKN and JMAT labs was supported by the Francis Crick Institute which receives its core funding from Cancer Research UK, the UK Medical Research Council, and the Wellcome Trust (FC001120 and FC001193).

Contributions

KKN conceived the project, designed and performed experiments, microinjected embryos and analysed data. NMEF performed single-cell analysis, hESC experiments, human and mouse embryo phenotyping and genotyping. AM performed genotyping of hESCs, stem cell derivation, mouse embryo phenotyping and generated the sgRNAs. KES generated the inducible hESCs, independently performed hESC phenotyping and performed flow cytometry analysis. AB designed and assisted with hESCs experiments and LV and AB supervised the experiments. NK and DW performed cytogenetic analysis and independently confirmed human embryo genotyping analysis. KE coordinated donation of embryos to the research project. BP generated some of the sgRNAs used in the mouse and supplied sgRNA sequences. PB and JK performed the RNA-seq analysis. RL and SEW assisted with phenotyping. DK, and J-SK performed Digenome-seq analysis. VM assisted with genotyping. KKN, JT and NMEF wrote the manuscript with help from all of the authors. All authors assisted with experimental design, generated figures and/or commented on the manuscript.

Figure Legends

Figure 1: Screening sgRNAs targeting OCT4 in optimised inducible CRISPR/Cas9 knockout human embryonic stem cells (hESCs) and mouse embryos.

a, Schematic of the strategy used to induce sgRNA expression in hESCs. The CAG promoter drives constitutive expression of the Cas9 gene as well as the tetracycline-responsive repressor (tetR). The inducible H1-TO promoter drives expression of each sgRNA in the presence of tetracycline (TET). The two transgenic cassettes are each targeted to one of the *AAVS1* genomic safe harbour loci using zinc-finger nucleases (ZFN). (TO: tetracycline-responsive operator).

b, Immunofluorescence analysis of OCT4 (red) or PAX6 (green) and DAPI nuclear staining (blue) expression in hESCs after 4 days of sgRNA2b induction (+Tet). Scale bars, 100 μm.

c, Quantification of indel mutations detected at each sgRNA on-target site. One-way ANOVA compared to uninduced hESCs. $^{*}P<0.05$; $^{**}P<0.01$.

d, Immunofluorescence analysis for OCT4 (red), SOX17 (green) and DAPI nuclear staining (blue) in control, OCT4-null or mosaic mouse blastocysts 4 days following zygote microinjection. Scale bar, 100 μm.

e, Quantification of proportions of OCT4-null, mosaic or wild-type mouse blastocysts following microinjection of Cas9 mRNA plus sgRNA1-1, sgRNA1-2, sgRNA2b, or sgRNA4 or uninjected controls. Chi-squared test. Data are mean ± s.d. $^{*}P<0.05$; $^{**}P<0.01$; $^{****}P<0.0001$.

f, Quantification of proportions of OCT4-null, mosaic or wild-type mouse blastocysts following microinjection of the sgRNA2b/Cas9 ribonucleoprotein complex concentrations indicated. Chi-squared test. Data are mean ± s.d. $^{****}P<0.0001$.

g, Comparison of mutation spectrums after targeting mouse embryos with sgRNA2b plus Cas9 mRNA or protein. Data are the proportion of unique indels observed. Chi-squared test. $^{****}P<0.0001$

Figure 2: The developmental potential of human embryos following CRISPR/Cas9-mediated genome editing.

a, Schematic of the first cell division in human embryos and time of microinjection. (PN, pronuclei; PNF, pronuclear fading).

b, Representative human embryo at each developmental stage analysed. (SC, start of cavitation; SB, start of blastocyst formation; B, blastocyst).

c, Morphokinetic analysis of human development after microinjection. Non-parametric two-tailed Kolmogorov-Smirnov test; ns, not significant.

d, Kaplan–Meier survival curve of human embryos following microinjection of Cas9 protein or sgRNA2b/Cas9 ribonucleoprotein complex. Zygotic *POU5F1* expression is initiated between the 4- to 8-cell stage. Chi-squared test. $^{*}P < 0.05$.

e, Karyotype analysis by whole genome sequencing of human blastocysts following microinjection of Cas9 protein or sgRNA2b/Cas9 ribonucleoprotein complex. Representative karyotypically normal embryos are shown.

Figure 3: Genotypic characterisation of OCT4-targeted human embryos.
a, Proportion of *POU5F1*-null, heterozygous or wild-type cells in each human embryo. The number of cells analysed is indicated. Embryos 2, 5, 7 and 8 were microinjected with Cas9 protein as a control. All other embryos were microinjected with the sgRNA2b/Cas9 ribonucleoprotein complex. The development of some embryos was stopped and they were removed from culture for analysis, while others were analysed following cleavage arrest.

b, The type and relative proportion of indel mutations observed compared to all observable indel mutations within each human embryo.

c, Immunofluorescence analysis for OCT4 (green), and DAPI nuclear staining (blue) in an uninjected control cleavage stage human embryo or an embryo that developed following sgRNA2b/Cas9 ribonucleoprotein complex microinjection ($n = 5$). Confocal z-section. Arrow, OCT4 expressing cell. Scale bar, 100 μm.

d, Immunofluorescence analysis for OCT4 (green), SOX17 (red) and DAPI nuclear staining (blue) in an uninjected control human blastocyst ($n = 3$) or a blastocyst that developed following sgRNA2b/Cas9 ribonucleoprotein complex microinjection ($n = 3$). Confocal z-section. Scale bar, 100 μm.

e, Quantification of the number of DAPI or OCT4 positive nuclei in uninjected control human blastocysts ($n = 3$) compared to blastocysts that developed following sgRNA2b/Cas9 ribonucleoprotein complex microinjection ($n = 5$). One-tailed t-test. $^{**}P < 0.01$; $^{***}P < 0.001$.

Figure 4: Phenotypic characterisation of OCT4 targeted human embryos.
a, Principal component analysis of single-cell RNA-seq data showing comparisons between the cells from human blastocysts that developed following microinjection of the sgRNA2b/Cas9 ribonucleoprotein complex (filled shapes) compared to Cas9 protein microinjected controls (unfilled shapes). The genotype of each cell is distinguished by colour. 5 samples failed repeated genotyping but the RNA quality is good and these are listed as Unknown. Each data point represents a single cell.

b, Immunofluorescence analysis for OCT4 (green), NANOG (red) and DAPI nuclear staining (blue) in a human or a mouse uninjected control blastocyst or a blastocyst that developed following sgRNA2b/Cas9 ribonucleoprotein complex microinjection (mouse: $n = 7$; human: $n = 3$). Confocal z-section. Scale bar, 100 μm.

c, Immunofluorescence analysis for OCT4 (green), GATA2 (magenta) and DAPI nuclear staining (blue) in an uninjected control human blastocyst (n = 3) or in a blastocyst that developed following sgRNA2b/Cas9 ribonucleoprotein complex microinjection (n = 3). Confocal projection. Scale bar, 100 μm.

d, Immunofluorescence analysis for OCT4 (green), ZO-1 (magenta) and DAPI nuclear staining (blue) in an uninjected control human blastocyst (n = 2) or in a blastocyst that developed following sgRNA2b/Cas9 ribonucleoprotein complex microinjection (n = 2). Confocal projection. Scale bar, 100 μm.

e, Principal component analysis of a previously published human single-cell RNA-seq dataset[30] integrated with the data from the Cas9 protein control and the sgRNA2b/Cas9 ribonucleoprotein (RNP) microinjected embryos. Each point represents a single cell.

f, Diagram summarising the observations made in the study and their relationship to the onset of zygotic *POU5F1* expression.

References

1 Chen, A. E. *et al.* Optimal timing of inner cell mass isolation increases the efficiency of human embryonic stem cell derivation and allows generation of sibling cell lines. *Cell Stem Cell* **4**, 103-106, doi:10.1016/j.stem.2008.12.001 (2009).

2 Niakan, K. K. & Eggan, K. Analysis of human embryos from zygote to blastocyst reveals distinct gene expression patterns relative to the mouse. *Dev Biol* **375**, 54-64, doi:10.1016/j.ydbio.2012.12.008 (2013).

3 Blakeley, P. *et al.* Defining the three cell lineages of the human blastocyst by single-cell RNA-seq. *Development* **142**, 3613, doi:10.1242/dev.131235 (2015).

4 Jinek, M. *et al.* A programmable dual-RNA-guided DNA endonuclease in adaptive bacterial immunity. *Science* **337**, 816-821, doi:10.1126/science.1225829 (2012).

5 Kang, X. *et al.* Introducing precise genetic modifications into human 3PN embryos by CRISPR/Cas-mediated genome editing. *J Assist Reprod Genet* **33**, 581-588, doi:10.1007/s10815-016-0710-8 (2016).

6 Tang, L. *et al.* CRISPR/Cas9-mediated gene editing in human zygotes using Cas9 protein. *Mol Genet Genomics* **292**, 525-533, doi:10.1007/s00438-017-1299-z (2017).

7 Liang, P. *et al.* CRISPR/Cas9-mediated gene editing in human tripronuclear zygotes. *Protein Cell* **6**, 363-372, doi:10.1007/s13238-015-0153-5 (2015).

8 Ma, H. *et al.* Correction of a pathogenic gene mutation in human embryos. *Nature*, doi:10.1038/nature23305 (2017).

9 Frum, T. *et al.* Oct4 cell-autonomously promotes primitive endoderm development in the mouse blastocyst. *Dev Cell* **25**, 610-622, doi:10.1016/j.devcel.2013.05.004 (2013).

10 Nichols, J. *et al.* Formation of pluripotent stem cells in the mammalian embryo depends on the POU transcription factor Oct4. *Cell* **95**, 379-391 (1998).

11 Bertero, A. *et al.* Optimized inducible shRNA and CRISPR/Cas9 platforms for in vitro studies of human development using hPSCs. *Development* **143**, 4405-4418, doi:10.1242/dev.138081 (2016).

12 Hsu, P. D. *et al.* DNA targeting specificity of RNA-guided Cas9 nucleases. *Nat Biotechnol* **31**, 827-832, doi:10.1038/nbt.2647 (2013).

13 Niwa, H., Masui, S., Chambers, I., Smith, A. G. & Miyazaki, J. Phenotypic complementation establishes requirements for specific POU domain and generic

transactivation function of Oct-3/4 in embryonic stem cells. *Mol Cell Biol* **22**, 1526-1536 (2002).

14 Scholer, H. R., Ruppert, S., Suzuki, N., Chowdhury, K. & Gruss, P. New type of POU domain in germ line-specific protein Oct-4. *Nature* **344**, 435-439, doi:10.1038/344435a0 (1990).

15 Kim, D. *et al.* Digenome-seq: genome-wide profiling of CRISPR-Cas9 off-target effects in human cells. *Nat Methods* **12**, 237-243, 231 p following 243, doi:10.1038/nmeth.3284 (2015).

16 Kim, D., Kim, S., Kim, S., Park, J. & Kim, J. S. Genome-wide target specificities of CRISPR-Cas9 nucleases revealed by multiplex Digenome-seq. *Genome Res* **26**, 406-415, doi:10.1101/gr.199588.115 (2016).

17 Wang, H. *et al.* One-step generation of mice carrying mutations in multiple genes by CRISPR/Cas-mediated genome engineering. *Cell* **153**, 910-918, doi:10.1016/j.cell.2013.04.025 (2013).

18 Le Bin, G. C. *et al.* Oct4 is required for lineage priming in the developing inner cell mass of the mouse blastocyst. *Development* **141**, 1001-1010, doi:10.1242/dev.096875 (2014).

19 Yen, S. T. *et al.* Somatic mosaicism and allele complexity induced by CRISPR/Cas9 RNA injections in mouse zygotes. *Dev Biol* **393**, 3-9, doi:10.1016/j.ydbio.2014.06.017 (2014).

20 Cho, S. W., Lee, J., Carroll, D., Kim, J. S. & Lee, J. Heritable gene knockout in Caenorhabditis elegans by direct injection of Cas9-sgRNA ribonucleoproteins. *Genetics* **195**, 1177-1180, doi:10.1534/genetics.113.155853 (2013).

21 Shin, H. Y. *et al.* CRISPR/Cas9 targeting events cause complex deletions and insertions at 17 sites in the mouse genome. *Nat Commun* **8**, 15464, doi:10.1038/ncomms15464 (2017).

22 Capmany, G., Taylor, A., Braude, P. R. & Bolton, V. N. The timing of pronuclear formation, DNA synthesis and cleavage in the human 1-cell embryo. *Mol Hum Reprod* **2**, 299-306 (1996).

23 Balakier, H., MacLusky, N. J. & Casper, R. F. Characterization of the first cell cycle in human zygotes: implications for cryopreservation. *Fertil Steril* **59**, 359-365 (1993).

24 Kim, S., Kim, D., Cho, S. W., Kim, J. & Kim, J. S. Highly efficient RNA-guided genome editing in human cells via delivery of purified Cas9 ribonucleoproteins. *Genome Res* **24**, 1012-1019, doi:10.1101/gr.171322.113 (2014).

25 Vera-Rodriguez, M., Chavez, S. L., Rubio, C., Reijo Pera, R. A. & Simon, C. Prediction model for aneuploidy in early human embryo development revealed by single-cell analysis. *Nat Commun* **6**, 7601, doi:10.1038/ncomms8601 (2015).

26 Wells, D. *et al.* Clinical utilisation of a rapid low-pass whole genome sequencing technique for the diagnosis of aneuploidy in human embryos prior to implantation. *J Med Genet* **51**, 553-562, doi:10.1136/jmedgenet-2014-102497 (2014).

27 Maurer, M. *et al.* Chromosomal Aneuploidies and Early Embryonic Developmental Arrest. *Int J Fertil Steril* **9**, 346-353 (2015).

28 Wong, C. C. *et al.* Non-invasive imaging of human embryos before embryonic genome activation predicts development to the blastocyst stage. *Nat Biotechnol* **28**, 1115-1121, doi:10.1038/nbt.1686 (2010).

29 Macaulay, I. C. *et al.* G&T-seq: parallel sequencing of single-cell genomes and transcriptomes. *Nat Methods* **12**, 519-522, doi:10.1038/nmeth.3370 (2015).

30 Yan, L. *et al.* Single-cell RNA-Seq profiling of human preimplantation embryos and embryonic stem cells. *Nat Struct Mol Biol* **20**, 1131-1139, doi:10.1038/nsmb.2660 (2013).

31 Roode, M. *et al.* Human hypoblast formation is not dependent on FGF signalling. *Dev Biol* **361**, 358-363, doi:10.1016/j.ydbio.2011.10.030 (2012).

32 Kuijk, E. W. *et al.* The roles of FGF and MAP kinase signaling in the segregation of the epiblast and hypoblast cell lineages in bovine and human embryos. *Development* **139**, 871-882, doi:10.1242/dev.071688 (2012).
33 Suzuki, T., Asami, M. & Perry, A. C. Asymmetric parental genome engineering by Cas9 during mouse meiotic exit. *Sci Rep* **4**, 7621, doi:10.1038/srep07621 (2014).

Extended Data Figure Legends

Extended Data Figure 1: *POU5F1* targeting and comparison of sgRNAs

a, Schematic representation of the human *POU5F1*/OCT4 locus and sgRNA targeting sites. The location (not to scale) and sequences of the sgRNAs tested are shown and the protospacer-adjacent motif (PAM) sequences are underlined and in red font. Sequences within the exons are in uppercase and introns are in lowercase. The mouse sgRNA sequences are shown below. The exons encoding the N-terminal domain (NTD), POU DNA binding domain or the C-terminal domain (CTD) are indicated.

b, Representative flow cytometry analysis quantifying OCT4 expression in hESCs induced to express each sgRNA over 5 days compared to uninduced controls. The percentage of OCT4 protein expression is shown.

c, qRT-PCR analysis after 4 days of sgRNA induction. Relative expression reflected as fold difference over uninduced cells normalised to *GAPDH*. Data points and mean for all samples are shown: $n = 2$ sgRNA1-1 clones; $n = 3$, sgRNA 1-2, 2b or 4 clones, representative of two independent experiments and ± s.e.m. where there are three samples. Two-way ANOVA. $^{*}P<0.05$; $^{**}P<0.01$; $^{***}P<0.001$; $^{****}P<0.0001$.

d, Heat maps of selected genes showing unsupervised hierarchical clustering of uninduced and sgRNA2b-induced hESCs. Normalised RNA-seq expression levels are plotted on a high-to-low scale (purple-white-green).

Extended Data Figure 2: Further characterisation of sgRNA2b-induced hESCs.

a, hESCs induced to express sgRNA2b for 4 days (+Tet) in chemically defined media with activin A and FGF2 (CDM/AF) compared to uninduced controls (No Tet). Immunofluorescence analysis for pluripotency markers OCT4, NANOG and SOX2 or markers associated with differentiation to early derivatives of the germ layers (SOX1-expressing ectoderm cells or SOX17-expressing endoderm cells). DAPI nuclear staining (blue) is shown. Scale bar, 400 μm.

b, qRT-PCR analysis for selected genes associated with either pluripotency or differentiation to derivatives of the germ layers in hESCs induced to express each of the sgRNA for 4 days. Relative expression reflected as fold difference over wild-type hESCs and normalised to *PBGD*. Data points and mean for all samples are shown: $n = 2$ sgRNA1-1 clones; $n = 3$, sgRNA 1-2, 2b or 4 clones, representative of two independent experiments and ± s.e.m. where there are three samples. Two-way ANOVA. $^{*}P<0.05$; $^{**}P<0.01$; $^{***}P<0.001$; $^{****}P<0.0001$, ns, not significant.

Extended Data Figure 3: On-target mutation spectrum in hESCs induced to express sgRNA1-1, sgRNA1-2, sgRNA2b or sgRNA4.

Shown are frequent types of indel mutations and corresponding sequences observed in hESCs induced to express sgRNA1-1, sgRNA1-2, sgRNA2b or sgRNA4. The cells were induced to express each sgRNA for 4 days and the data shown is representative of the type of indel

mutations observed in other clonal lines (n = 2 sgRNA1-1 clones; n = 3, sgRNA 1-2, 2b or 4 clones) and across time (from 1 up to 4 days following induction of each sgRNA).

Extended Data Figure 4: Off-target analysis of sgRNA2b-induced hESCs.

a, The *POU5F1* sgRNA2b 12 bp seed sequence is highlighted in green and the NGG PAM sequence in red. In black are the nucleotide sequences 5' to the sgRNA seed sequence. 7 putative off-target sequences and associated genes are shown including *POU5F1* pseudogenes. In orange are the nucleotides that differ from the sgRNA2b sequence.

b, Percentage of indel mutations detected at putative off-target sites in hESCs 4 days following tetracycline induction of sgRNA2b compared to uninduced controls. Data are percentages of indels detected in the cell lines at each of the sites indicated. Comparisons made between three clonal hESC lines induced to express sgRNA2b versus uninduced controls. The percentage of indel mutations induced at the on-target site were significant while all other sites were not significantly different. Two-way ANOVA. $^{***}P<0.001$.

c, Digenome-seq results displayed as a genome-wide circos plot. The height of the peak corresponds to the DNA cleavage score. The red arrow points to the *POU5F1* locus on chromosome 6.

d, Percentage of indel mutations observed in sgRNA2b-induced hESCs and in wild-type H9 control cells at each locus following targeted deep sequencing of putative off-target sites identified by Digenome-seq.

e, Off-target candidate nucleotides displayed as sequence logos using the WebLogo program.

f, Percentage of indel mutations observed in sgRNA2b-induced hESCs and in wild-type H9 control cells following targeted deep sequencing of putative off-target sites determined by WebLogo sequence homology.

Extended Data Figure 5: Assessing a range of Cas9 and sgRNA combinations for microinjection into mouse pronuclear zygotes.

Additional conditions were tested in mouse embryos microinjected with the sgRNA2b either **a,** plus Cas9 mRNA or

b, as a complex with the Cas9 protein at the ratios indicated. Quantification was performed on the proportion of mouse embryos at the blastocyst stage that are phenotypically null (loss of OCT4 and SOX17 protein expression), mosaic/heterozygous (partial OCT4 and/or SOX17 expression) or uninjected (strong OCT4 and SOX17 expression). Data are mean ± s.d. and comparisons made between the percentage of *OCT4*-null embryos observed versus wild-type uninjected control embryos. Chi-squared test. $^{*}P<0.05$; $^{***}P<0.001$; $^{****}P<0.0001$.

c, The type of indel mutations detected in mouse embryos microinjected with the sgRNA2b/Cas9 ribonucleoprotein complex. The sgRNA sequence is boxed and the NGG PAM site underlined. Dash, deletion position.

d, Further characterization of mouse embryos microinjected with sgRNA2b/Cas9 ribonucleoprotein complex compared to uninjected control blastocysts. Immunofluorescence analysis for markers of the trophectoderm (CDX2) or primitive endoderm (GATA4, GATA6, PDGFRA and SOX7) lineages together with DAPI nuclear staining. Confocal z-section. Scale bar, 100 μm.

e, Quantification of blastocyst inner cell mass (ICM) or trophoblast outgrowths in mouse embryonic stem cell derivation conditions. Uninjected, Cas9-injected or Cas9 plus Dmc1 sgRNA (targeting a gene not essential for preimplantation development) were used as controls. Comparisons were made to blastocysts that developed following sgRNA2b/Cas9 ribonucleoprotein microinjection. Two-tailed t-test. $^{*}P<0.05$.

Extended Data Figure 6: Further assessing human embryo quality.

a, Karyotype analysis following whole genome sequencing of either single blastomeres or trophectoderm biopsies. Multiple biopies were analysed from embryos C8, C12 and C16. Analysis was also performed on blastocysts that developed following microinjection of Cas9. The type of chromosome gains and losses are indicated.

b, Representative karyotype analysis by whole genome sequencing of human blastocysts. A representative graph indicating aneuploidy in embryos following either Cas9 protein or sgRNA2b/Cas9 ribonucleoprotein complex microinjection.

c, Phase-contrast images of blastocysts that developed following microinjection of the sgRNA2b/Cas9 ribonucleoprotein complex compared to Cas9 protein injected controls. White arrows point to the presumptive inner cell mass and a black arrow to a representative zona pelucida.

Extended Data Figure 7: Evaluating on-target and putative off-target mutations in human embryo cells.

a, The type and relative proportion of indel mutations observed compared to all observable indel mutations within each human embryo.

b, Quantification of indels by TIDE analysis. Representative plots and Sanger sequencing chromatograms are shown from *OCT4*-null, heterozygous and wild-type human cells.

c, Percentage of indel mutations detected at the sgRNA2b on-target site and putative off-target sites in single cells microdissected from Cas9 protein microinjected control blastocysts or blastocysts that developed following sgRNA2b/Cas9 ribonucleoprotein complex microinjection. Putative off-target sites were evaluated in cells that were previously determined to be *OCT4*-null (green), heterozygous (orange) or wild-type (blue) along with samples from Cas9 protein microinjected embryos (red). Three representative examples are shown from each group.

d, Sanger sequencing chromatograms from *OCT4*-null single cells collected from human blastocysts that developed following sgRNA2b/Cas9 ribonucleoprotein complex microinjections. The chromatograms exemplify the sequence detected in all of the other samples analysed. Underlined is the sequence of the putative off-target site.

Extended Data Figure 8: Phenotypic characterisation of OCT4-targeted embryos.

a, Immunofluorescence analysis for OCT4 (green) and DAPI nuclear staining (blue) in human cleavage stage embryos following sgRNA2b/Cas9 ribonucleoprotein complex microinjection ($n = 5$). Confocal z-section. Arrow, OCT4 expressing cell. Scale bar, 100 μm.

b, Immunofluorescence analysis for OCT4 (green), SOX17 (red) and DAPI nuclear staining (blue) in an uninjected control blastocyst ($n = 3$) or a human blastocyst that developed following sgRNA2b/Cas9 ribonucleoprotein complex microinjection ($n = 3$). Confocal z-section. Scale bar, 100 μm.

c,d Immunofluorescence analysis for OCT4 (green), NANOG (red) and DAPI nuclear staining (blue) in **(c)** a human blastocyst that developed following sgRNA2b/Cas9 ribonucleoprotein complex microinjection (n = 3) or **(d)** in a mouse uninjected control blastocyst or in blastocysts that developed following sgRNA2b/Cas9 ribonucleoprotein complex microinjection (n = 7). Confocal z-section. Scale bar, 100 μm.

g, Quantification of NANOG and OCT4 expression in mouse uninjected control blastocysts (n = 5) or in blastocysts that developed following sgRNA2b/Cas9 ribonucleoprotein complex microinjection (n = 7). One-tailed t-test. $^{**}P<0.01$.

h, Immunofluorescence analysis for GATA2 (green) and DAPI nuclear staining (blue) in a human blastocyst that developed following sgRNA2b/Cas9 ribonucleoprotein complex microinjection (n = 3). Confocal projection. Scale bar, 100 μm.

Extended Data Figure 9:
a, Hierarchical clustering and heat map of a selection of genes following single cell RNA-seq analysis of human embryos. Embryos C8, C9, C12 and C16 (samples denoted in orange font) were targeted with the sgRNA2b/Cas9 ribonucleoprotein complex. Embryos 2, 5, 7 and 8 were microinjected with Cas9 protein as a control. An uninjected control reference dataset labelled PE (primitive endoderm cells), EPI (epiblast cells) or TE (trophectoderm cells) is included[3]. Control cells clustered according to lineage and are indicated with the coloured bars: red = PE, green = EPI and blue = TE. Grey bar highlights the samples that have low expression of markers of each of the lineages shown. The genotype of the samples are noted as *POU5F1* wild-type: WT, heterozygous: Het, or knockout: KO cells. 5 samples failed repeated genotyping but the RNA quality is good and these are listed as X. Normalised expression levels are plotted on a high-low scale (purple-white-green).

b,c Principal component analysis of a previously published human single-cell RNA-seq dataset[30] integrated with the data from the Cas9 protein control and the sgRNA2b/Cas9 ribonucleoprotein (RNP) microinjected embryos. Each point represents a single cell. Data were plotted along the **(b)** second and third or the **(c)** first and third principal components.

Extended Data Figure 10: Reagents list
a, Oligonucleotides used for cloning, MiSeq or qRT-PCR analysis

b, Antibodies used for immunofluorescence and flow cytometry analysis

METHODS

Ethics statement

This study was approved by the UK Human Fertilisation and Embryology Authority (HFEA): research licence number R0162 (http://www.hfea.gov.uk/docs/07032016_Currently_licenced_research_projects.pdf) and the Health Research Authority's Research Ethics Committee (Cambridge Central reference number 16/EE/0067).

The process of approval entailed independent peer review along with approval from both the HFEA Executive Licensing Panel (8 members of the Authority) and the Executive Committees, which is composed of 5 members including members of the lay public. Our research is compliant with the HFEA Code of Practice and has undergone independent inspections by the HFEA since the licence was granted. The Research Ethics Committee is

comprised of 12 individuals including members of the lay public. Patient consent was obtained from Bourn Hall Clinic.

Informed consent was obtained from all couples that donated spare embryos following IVF treatment. Before giving consent, people donating embryos were provided with all of the necessary information about the research project, an opportunity to receive counselling and the conditions that apply within the licence and the HFEA Code of Practice. Specifically, patients signed a consent form authorising the use of genome editing techniques including CRISPR/Cas9 on donated embryos. Donors were informed that after the embryos have been genetically modified their development will be stopped prior to 14 days post-fertilisation and that subsequent biochemical and genetic studies would be performed. Informed consent was also obtained from donors for all the results of these studies to be published in scientific journals. No financial inducements are offered for donation. The patient information sheets and consent document provided to patients are publicly available (https://www.crick.ac.uk/research/a-z-researchers/researchers-k-o/kathy-niakan/hfea-licence/). Embryos surplus to the patient's IVF treatment were donated cryopreserved and were transferred to the Francis Crick Institute where they were thawed and used in the research project.

Power analysis

The R statistical package pwr was used to determine the number of human embryos required to determine the function of OCT4 compared to microinjected controls. A two-sample t-test was performed to a significance level of $P<0.05$. The effect size was 0.8 which assumes an observable difference between the CRISPR injected and control embryos. The sample size was estimated to be 25 CRISPR-targeted embryos.

sgRNA design to target *POU5F1*

So as not to lower the targeting efficiency, we determined whether the sgRNAs targeted polymorphic regions of the human genome. Most sgRNA had a single nucleotide polymorphism (SNP) frequency of less than 0.1% in the human population, with the exception of the sgRNA targeting exon 4, which had a SNP frequency of 32% within the sgRNA target sequence as determined by the 1000 genomes project[34]. We retained this sgRNA as it had the highest *in silico* score and overlapped with a site that has been previously shown in complementarity studies to be functionally required for pluripotency, suggesting that even an in-frame deletion would render a loss of function in the gene [13]. We also favoured the use of sgRNAs with sequence conservation of the PAM and sgRNA seed sequence (approximately 12bp region proximal to the PAM sequence) that would allow us to determine efficiency in mouse embryos. In the case of high-scoring sgRNAs targeting exon 2d, there is no mouse equivalent sgRNA sequence that we could evaluate, and for exon 3, we could not design sgRNAs where the predicted cut site would be within the exon; these options were therefore excluded.

sgRNA production and ribonucleoprotein preparation

sgRNAs were prepared as previously described[35]. The sgRNA was cloned into the bicistronic expression vector px330 (Addgene; 42230[36]) using the Bbs1 restriction site. The sgRNA sequence from the correctly targeted px330 vector was amplified using the Q5 hot start high fidelity DNA polymerase (NEB; M0493) and the PCR product was *in vitro* transcribed using the MEGAshortscript T7 kit (ThermoFisher Scientific; AM1354) and purified using the Zymo RNA Clean & Concentrator columns (Zymo Research; R1017) The sgRNA and Cas9 mRNA (TriLink Biotechnologies; L61256) and recombinant Cas9 protein (Toolgen; TGEN CP1) were individually re-suspended in RNase-free water, aliquoted and stored at -80°C until use. Prior to injection the ribonucleoprotein complex was prepared by centrifuging the Cas9

protein for 1 min at 14,000 RPM at 4°C and transferring the supernatant to a fresh tube containing the sgRNA. This was incubated at 37°C for 15 min, pulse spun and transferred to a fresh tube for microinjection.

Mouse zygote collection

Four to eight-week-old (C57BL6 x CBA) F1 female mice were super-ovulated using injection of 5 IU of pregnant mare serum gonadotrophin (PMSG; Sigma-Aldrich). 48 h post PMSG, 5 IU of human chorionic gonadotrophin (HCG; Sigma-Aldrich) was administered. Superovulated females were set up for mating with eight-week-old or older (C57BL6 x CBA) F1 males. Mice were maintained on a 12 h light/dark cycle. Mouse zygotes were isolated in Global total with HEPES (LifeGlobal; LGTH-100) under mineral oil (Origio; ART-4008-5P) and cumulus cells were removed with hyaluronidase (Sigma-Aldrich; H4272). All animal research was performed in compliance with the UK Home Office Licence Number 70/8560.

Human embryo thaw

Human zygotes were thawed using Quinn's Advantage thaw kit (Origio; ART-8016). Briefly, upon thawing the embryos were transferred to 3 ml of 0.5% sucrose thawing medium and incubated for 5 min at 37°C, followed by 3 ml of 0.2% sucrose thawing medium for 10 min at 37°C. The embryos were then washed through 7 drops of diluent solution prior to culture. Human blastocysts were thawed using the Blast thaw kit (Origio; 10542010) following the manufacturer's instruction.

Human and mouse microinjection and culture

Human and mouse embryo microinjections were performed in Global Total media with HEPES under mineral oil on a heated stage with a holding pipet (Research Instruments) and a Femtojet 4i microinjection manipulator (Eppendorf) set at approximately 40 injection pressure and 20 constant pressure. Embryos were microinjected with a mixture of Cas9 mRNA+sgRNA or the ribonulceoprotein complex back-filled into microfilament glass capillary injection needles (World Precision Instruments; TW100F-6) pulled using a pipet puller (Suter; P-97 micropipette puller). The microinjection procedure took ~15 min to complete.

Human or mouse embryos were cultured in drops of pre-equilibrated Global media (LifeGlobal; LGGG-20) supplemented with 5 mg/mL protein supplement (LifeGlobal; LGPS-605) and overlaid with mineral oil (Origio; ART-4008-5P). Pre-implantation embryos were incubated at 37ºC and 5.5% CO_2 in an EmbryoScope+ time-lapse incubator (Vitrolife) for either 3 – 4 d (mouse) or 5-6 d (human).

Evaluating potential off-target sites

Putative off-targets were determined using the MIT CRISPR Design tool (crispr.mit.edu) which indicated top scoring off-target sites. We evaluated sequences that had mismatches of less than or equal to 3 nucleotides compared to the sgRNA2b sequence. As described previously[17] potential off-target sites were also identified by using the following parameters: 12 basepairs of the sgRNA seed sequence plus an NGG PAM sequence where (N was varied to include all possible nucleotides) were searched against the reference human genome (hg19).

Genomic DNA extraction

hESCs were lysed using proteinase K digestion (10 μg/ml in lysis buffer [100 mM Tris buffer pH 8.5, 5mM EDTA, 0.2% SDS, 200 mM NaCl]) overnight at 37°C. gDNA was extracted from the lysed cells using phenol:chloroform extraction followed by ethanol precipitation.

Genomic DNA from fixed embryos (human and mouse) was isolated using the alkaline lysis method; 25 µl of 50 mM NaOH was added to the sample and incubated at 95°C for 5 min. Samples were neutralized by adding 2.5 µl of 1M Tris-HCL pH 8.0.

The Illustra Single Cell GenomiPhi DNA Amplification Kit (GE Healthcare Life Sciences; 29108039) was used according to manufacturer's instructions to amplify gDNA from unfixed mouse blastocysts. DNA was purified by adding 30 ul of 20 mM EDTA, 5 µl of 3 M sodium acetate and 137 µl ice cold ethanol. Tubes were mixed by inverting and centrifuged at 16,000 x g for 20 min. Supernatant was removed and DNA was washed in 100 µl ice cold 70% ethanol by mixing and centrifuging for 5 min. DNA was resuspended by adding 20 µl H_2O and incubating for 20 min at 4ºC before mixing by gentle pipetting.

Genomic DNA from single cells microdissected from human embryos was extracted using the G+T-protocol and amplified using REPLI-g Single Cell Kit (Qiagen; 150343) according to manufacturer's guidelines. In preparation for PCR amplification and MiSeq analysis the WGA-DNA product was diluted 1:100 in nuclease-free water, and 2 µl of this was used as the template in a reaction containing 25 µl Phusion High Fidelity PCR Master Mix (New England Biolabs), 2.5 µl 5 µM forward primer, 2.5 µl reverse primer and 18 µl nuclease-free water. Thermocycling settings used were as follows: 98 ºC 30 sec, 35 cycles of 98 ºC 10 sec, 58 ºC 30 sec, 72 ºC 30 sec, and a final extension of 72 ºC for 5 min. PCR amplicons were analysed by Sanger sequencing and indels were quantified by TIDE webtool[37].

On- and off-target sites were amplified using primers listed in Extended Data Fig. 10a using the GC rich PCR system (Sigma-Aldrich; 12140306001). Primers were designed to generate amplicons of approximately 250 bp centered around the predicted cute site so as to maximize the detection of a variety of mutations and ensure that each amplicon was sequenced continuously from the forward and reverse barcode. We excluded primers that had SNPs within their sequence so as to prevent allelic drop out. For the time-course genotypic analysis bulk cells were collected every 24 h and PCR products were amplified from the extraction genomic DNA. These products were used to generate multiplexed libraries for targeted amplicon sequencing by MiSeq according to the manufacturer's instructions (Illumina).

For gDNA amplified through the G+T-seq protocol, amplicons for genotyping were generated using Phusion High Fidelity PCR Master Mix (New England Biolabs). Miseq library preparation, quantification, pooling and denaturation were performed according to the manufacturer's instructions (Illumina). For low input samples amplicons were cleaned using an equal volume of AMPure XP beads according to manufacturer's instructions (Beckman Coulter) Index PCR was performed using 10 µl of cleaned amplicon, 12.5 µl Q5 high fidelity 2X Master Mix (NEB; M0492S), 1.25 µl Nextera XT Index 1 primer, 1.25 µl Nextera XT Index 2 primer (Nextera XT Index kit; FC-131-1001). The thermocycling parameters used were: 98°C for 30 sec, 35 cycles of 98°C for 10 sec, optimized annealing temperature for 30 sec, 72°C for 30 sec, and a final extension of 72°C for 2 min. Index PCR was cleaned using equal volume of AMPure XP beads as described previously. Beads were rehydrated with 20 µl nuclease-free water. 5 µl of the index PCR product was run on a gel to identify any samples with over-abundance of primer dimers, which were subsequently subjected to gel size selection and extraction using QIAquick gel extraction kit (Qiagen; 28704). Index PCR products were quantified using QuantiFluor dsDNA system (Promega; E2670). The concentration was used to determine the dilution required to obtain a 5 µM solution of each sample. 5 µl of each sample was pooled and the library was spiked with 20% PhiX genomic control (Illumina; FC-110-3001). Sequencing generated paired-end (2 x 250 bp) dual indexed reads. After sequencing, reads were demultiplexed and stored as FASTQ files for downstream

processing and analysis. The CRISPR Genome Analyser[38] or CRISPR Cas Analyser[39] tools were used to align the reads and to determine the percentage of non-wild-type reads resulting from editing, as well as assessing the position and size of each indel for all of the PCR amplicons evaluated.

Digenome sequencing

Digenome-seq was performed as described previously[15,16]. Briefly, 20 μg of genomic DNA was incubated with pre-incubated 100 nM recombinant Cas9 protein and 300 nM sgRNA in a reaction volume of 1 ml (100 mM NaCl, 50 mM Tris-HCl, 10 mM MgCl2, 100 μg/ml BSA, pH 7.9) at 37 °C for 8 h. Digested DNA was mixed with 50 μg/ml RNase A (Qiagen) at 37 °C for 30 min, and purified again with a DNeasy Tissue Kit (Qiagen). 1 μg of digested DNA was fragmented using the Covaris system and ligated with adaptors using TruSeq DNA libraries. DNA libraries were subjected to whole genome sequencing was performed at Macrogen using an Illumina HiSeq X Ten at a sequencing depth of 30–40X. *In vitro* DNA cleavage scores were calculated using a scoring system described previously[16].

Immunohistochemistry

Embryos and cells were fixed with 4% paraformaldehyde in PBS respectively for 1 h and overnight at 4^{o}C and immunofluorescently analysed as described previously[2]. The primary antibodies used are listed in Extended Data Fig. 10b. Embryos were placed on coverslip dishes (MatTek) for confocal imaging.

Cytogenetic analysis

To determine the chromosome copy number, single or multiple blastomeres were biopsied from embryos at the cleavage stage and clumps of approximately five cells were microdissected from blastocysts. The cells were washed through 3 drops of a wash buffer (PBS/0.1% polyvinyl alcohol), which had previously been tested to confirm absence of contaminating DNA (Reprogenetics UK). The cells were transferred to 0.2 ml PCR tubes in a volume of 1.5 uL, lysed and subjected to whole genome amplification (SurePlex, Rubicon) followed by low-pass next generation sequencing (coverage depth <0.1x) (VeriSeq PGS kit, Illumina). Libraries were prepared according to the manufacturer's instructions and sequenced using the MiSeq sequencing platform. Typically, ~1 million reads were generated per sample, of which 60-70% successfully mapped to unique genomic sites. Mapped reads were interpreted using BlueFuse Multi software (Illumina) in order to generate chromosome copy number profiles. This strategy has been extensively validated and is widely used for the detection of whole chromosome losses and gains, as well as segmental aneuploidy, in human embryos undergoing preimplantation genetic diagnosis (PGD)[26]. Analysis of single blastomeres allowed each chromosomal region of at least 5 Mb to be assigned a copy number of 0, 1, 2, 3 or 4 (corresponding to nullisomy, monosomy, disomy, trisomy or tetrasomy). In trophectoderm samples, composed of several cells, it was also possible to detect the presence of chromosomal mosaicism, indicated when copy number values for a given chromosome had an intermediate value, between the thresholds for assigning 1 and 2 or 2 and 3 chromosome copies[40].

Imaging

Confocal immunofluorescence pictures were taken with a Leica SP5 confocal microscope and 3 - 5 μm thick optical section were collected. Quantification was performed manually using Fiji (ImageJ) or automated using MINS 1.3 software[41].

Epifluorescence images were performed on an Olympus IX73 using Cell^F software (Olympus Corporation) or on an EVOS FL cell imaging system (AMF4300). Phase contrast

images and videos were performed on an Olympus IX73 using with Cell^F software and RI Viewer software (Research Instruments), respectively.

Time-lapse imaging was performed using an EmbryoScope+ time-lapse incubator (Vitrolife) and annotated using the EmbryoViewer software.

Culture conditions for hESCs and engineering inducible cell lines

Clonal H9 hESCs (WiCell) (n = 2 or 3 per sgRNA) were cultured in feeder- and serum-free conditions either in mTeSR1 (Stem Cell Technologies) on growth factor reduced Matrigel-coated dishes (BD Biosciences) or as previously described[42]. Successfully targeted cells were selected using 0.25 µg/ml puromycin (Sigma-Aldrich) and 15 µg/ml geneticin (Insight biotechnology ltd.) for 3 d prior to induction. Tetracycline hydrochloride (Sigma-Aldrich; T7660) was used at 1 µg/ml to induce guide expression. hESCs underwent routine mycoplasma screening and katyotyping.

Generation of optimized inducible knockout (OPTiKO) hESC lines

The sgRNA sequences were cloned into the pAAV-Puro_siKO-TO vector as previously described[11]. Briefly, complementary single stranded oligonucleotides (Extended Data Fig. 10a) were annealed and scarlessly ligated to AarI-digested plasmids between the H1-TO tetracycline-inducible promoters and the scaffold sgRNA sequence. The Cas9 and inducible sgRNA targeting vectors were each inserted into one of the two alleles of the *AAVS1* locus by homologous-directed recombination facilitated by two obligate heterodimer Zinc Finger Nucleases (ZFN)[11]. Cells were cultured in the presence of 10 µM ROCK inhibitor Y-27632 (Sigma-Aldrich; Y0503) in media without antibiotics 24 h prior to nucleofection. Cells were washed with PBS (Life Technologies; 14190-094) and dissociated with Accutase (Life Technologies; A11105-01) for 5 min at 37°C. Colonies were mechanically triturated into clumps of 2/3 cells and counted. $2x10^6$ cells were nucleofected in 100 µl with a total of 12 µg of DNA (4 µg each for the two ZFN plasmids, and 2 µg each for the two targeting vectors) using the Lonza P3 Primary Cell 4D-Nucleofector X Kit and the cycle CA-137 on a Lonza 4D-Nucleofector System. Cells were incubated for 5 min at RT, after which antibiotic-free KSR containing 10 µM ROCK inhibitor was added. After another 5 min the cell suspension was distributed on pre-plated DR4 (Applied Stem Cell; ASF-1013) drug resistant MEF feeders in antibiotic-free KSR media. Four days post nucleofection, cells underwent double antibiotic selection with 0.5 µg/ml Puromycin (Sigma-Aldrich) and 25 µg/ml Geneticin (G418 Sulfate (Gibco)) for 7 days. Targeted colonies appeared after 4-8 d and were mechanically picked and clonally expanded at 10-14 d after transfection.

Extensive genotyping was carried out on the targeted clones to check for correct AAVS1 gene targeting and to exclude the presence of randomly integrated plasmids, as previously described[11]. Briefly, genomic DNA was extracted using the Wizard Genomic DNA Purification Kit (Promega; A1120). Site-specific integration was checked for both 5'and 3'ends of each of the two targeting vectors (Cas9 and inducible sgRNA). Clones were also screened for the absence of the WT locus (indicating homozygous targeting) and for the absence of amplicons for both the 5' and 3' ends of the targeting vector backbones to ensure there was no random integration of the plasmid).

Flow cytometry

Cells were collected every day for 5 d alongside matched control cells. Cells were dissociated into single cell suspension using TrypLE Select 1X (Gibco; 12563011) for 5 min at 37°C. The cell suspension was pelleted, washed with PBS (Life Technologies; 14190-094) then fixed and permeabilized using BD Cytofix/Cytoperm (554714) for 20 min at 4°C. Perm/wash buffer (diluted 1:10 in embryo transfer water) was used for all subsequent antibody and wash steps

unless indicated otherwise. After fixation, cells were washed once then stored at 4°C until the d5 sample had been collected, at which point all samples underwent intracellular staining. Cells were blocked for 30 min at room temperature with perm/wash buffer containing 10% donkey serum (Bio-rad; C06SB) and 0.1% Triton X-100 (ThermoFisher Scientific; 85111). Cells were stained with primary antibodies by incubating at RT for 1 h and cells were washed three times following each incubation. Negative control secondary only stained cells and unstained cells were performed on each batch of cells at a given day. Flow cytometry was performed using a Cyan ADP flow cytometer and the Summit software (Beckman Coulter), and 10,000-50,000 events were recorded. Flow cytometry result analysis was performed using FlowJo. Cells were first gated based on forward and side scatter properties, after which singlets were isolated based on the relationship between side scatter area peak area and width. A secondary only negative control was used to determine the background and OCT4 positive cells were quantified relative to cells that were OCT4 negative in the total bulk population of cells analysed.

RNA isolation from hESCs for RNA-seq and qRT-PCR

qRT-PCR data presented in Extended Data Fig. 1c was generated as follows: RNA was isolated using TRI reagent (Sigma) and DNase I-treated (Ambion). cDNA was synthesized using a Maxima first strand cDNA synthesis kit (Fermentas). qRT-PCR was performed using SensiMix SYBR low-ROX kit (Bioline) on a QuantStudio 5 machine (ThermoFisher Scientific). Primers pairs used are listed in the Extended Data Fig. 10a. Each sample was run in triplicate and samples were normalized using *GAPDH* as the housekeeping gene and the results were analysed using the ΔΔCt method

In preparation for RNA-sequencing of the hESCs induced to express sgRNA2b, samples were further cleaned using ethanol precipitation. Libraries were prepared using KAPA mRNA HyperPrep kit for Illumina platforms (Roche Sequencing Solutions Inc.)

qRT-PCR data presented in Extended Data Fig. 2b was generated as follows: RNA was extracted using the GenElute Mammalian Total RNA Miniprep Kit (Sigma-Aldrich; RTN350-1KT) and the On-Column DNAse I Digestion kit (Sigma-Aldrich; DNASE70-1SET). 500 ng of RNA was reverse transcribed with SuperScript II (Invitrogen; 18064071). qPCR was performed using 5 ng of cDNA and SensiMix SYBR low-ROX (Bioline; QT625-20). qRT-PCR was performed on a Stratagene Mx-3005P (Agilent Technologies) and the results were analysed using the ΔΔCt method. Each sample was run in duplicate and samples were normalized using *RPLP0* as the housekeeping gene.

G&T-seq

Samples were processed using a previously published protocol that was adapted where indicated[29]. Single cells from microdissected human embryos were picked using 100 µm inner diameter Stripper pipette (Origio) and transferred to individual low bind RNAse-free tubes containing 2.5 µl RLP plus buffer (Qiagen; 79216).

To separate RNA and genomic DNA (gDNA) 50 µl of Dynabeads were washed and incubated with 100 uM biotinylated poly-dT oligonucleotide (IDT). 10 µl of oligo-dT beads were added to each tube containing the single cell. Samples were incubated in a thermomixer for 20 min at room temperature at 2000 rpm. Tubes were put on a magnet until the beads collected into a pellet and the supernatant went clear. The supernatant containing the gDNA was transferred to a new collection tube. Beads were washed three times to collect any residual gDNA.

cDNA was generated from the RNA captured on the bead using the SMARTer v4 Ultra Low Input kit (Clontech; 634891) as previously described[3]. Reverse transcription was performed

on the thermomixer using the settings 2 min at 42°C at 2,000 rpm, 60 min at 42°C at 1,500 rpm, 30 min at 50°C at 1,500 rpm and 10 min at 60°C at 1,500 rpm. cDNA was amplified by adding 12.5 µl 2X SeqAmp PCR buffer, 0.5 µl PCR Primer II A (12µM), 0.5 µl SeqAmp DNA polymerase, 1.5 µl Nuclease free water. Beads were mixed on thermomixer for 60 sec at room temperature at 2,000 rpm and then were incubated on a PCR machine using the following settings: 95°C for 1 min, 24 cycles of 98°C for 10 sec, 65°C for 30 sec and 68°C for 3 min, before a final extension for 10 min at 72°C. Amplified cDNA was purified by adding 25 µl Ampure XP beads according to manufacturer's instructions. 12 µl of purification buffer was added to rehydrate the pellet and incubated for 2 min at room temperature. cDNA was eluted by pipetting up and down 10 times before returning the tube to the magnet. The clear supernatant containing the cDNA was removed from the immobilised beads and transferred to a new low-bind tube. cDNA was stored at -80°C until library preparation. cDNA quality was assessed by High Sensitivity DNA assay on an Agilent 2100 Bioanalyser with good quality cDNA showing a broad peak from 300 to 9,000 bp. cDNA concentration was measured using QuBit dsDNA HS kit (Life Technologies).

In preparation for library generation cDNA was sheared using an E220 focused-ultrasonicator (Covaris) to achieve cDNA in 200-500 bp range. 10 µl of cDNA sample and 32 µl purification buffer was added to Covaris AFA Fiber Pre-Slit Snap Cap microTUBE. cDNA was sheared using the following settings: Peak Incident power 175 W, Duty Factor 10%, 200 cycles per burst, water level 5.

Libraries were prepared using Low Input Library Prep Kit v2 (Clontech; 634899) according to manufacturer's instructions. Dual indexing was performed by substituting the manufacturer's provided indexing adaptors with NEBNext Multiplex Oligos for Illumina Dual Index primers set 1 (NEB; E7600S). Library quality was assessed by Bioanalyser and the concentration was measured by high sensitivity QuBit assay.

25 µl of AMPure beads was added to each collection tube containing the gDNA. Tubes were mixed well and incubated at room temperature for 20 min so that the DNA could be bound to the beads. Tubes were put on the magnet until the supernatant ran clear so that it could be removed and discarded. The beads were washed twice with 100 µl 80% ethanol. Any remaining ethanol was removed and beads allowed to dry.

Genotyping cells from human embryos

PCR amplification of the sgRNA2b on-target site was initially performed on all samples using a primer pair generating an amplicon size of 244 bp suitable for MiSeq analysis. Any samples which failed three times to amplify using this primer pair were subjected to amplification using alternative primer pairs listed in Extended Data Fig. 10a. Putative off-target sites were evaluated using the primer pairs listed in Extended Data Fig. 10a.

Single-cell RNA-seq data analysis

RNA-Seq data of single cells were obtained as paired-end reads and analysis was performed blinded to the identity of the samples. The RNA-Seq data flow was managed by a GNU make pipeline. Transcript reads were aligned to the Ensembl GRCh37 genome using Tophat2 (version 2.1.1 with option no coverage search)[43]; alignment rates were typically between 60-80%. Transcript counts were computed using the featureCounts program (version 1.5.1)[44]. A quality filter was applied to the matrix, ensuring >50000 total transcript reads per cell and >5 reads in at least 5 samples. The raw transcript counts were corrected for read-count depth effects using the SCnorm package[45] single-group design matrix. The RUVSeq[46] (version 1.10.0) (Risso et al. 2014) was used for between-sample normalisation by applying the 'betweenLaneNormalization' function with 'full' quantile regression. For PCA analysis,

transcript counts were transformed using a asinh(x/2) transformation with per-gene centering to obtain near-Gaussian and zero-centred count distributions. The prcomp function of the stats package in R (version 3.4.1) was applied to the count matrix and single cells were projected into the plane of the first two eigenvectors.

Independently, sequenced reads from all single cell samples were also aligned to the human reference genome sequence GRCh38 using TopHat2 (version 2.1.1)[43] and parameters were optimised for 100bp paired-end reads. Read counts per gene were calculated using the python package HTSeq (version 0.6.1)[47] and differential gene expression analysis was carried out using DESeq2 (version 1.10.1)[48]. Read counts were normalised using the RPKM method[49] and hierarchical clustering of samples was performed to generate a heat map using the R package pheatmap (version 1.0.8). A previously published reference control dataset[3] was integrated in the heat map and hierarchical clustering. Principal components analysis was performed using the stats (version 3.2.2) R package on a previously published scRNA-seq dataset covering different stages of preimplantation development[30] together with own OCT4-targeted samples and controls.

Data availability

Source Data are provided for figures. RNA-seq and MiSeq data has been deposited into Gene Expression Omnibus under accession numbers (GSE100120). Scripts used for bioinformatics analysis can be found on the following GitHub page: https://github.com/Genalico/RNAseq-BlaCy_pub. Any additional information is available upon request from the corresponding author.

34 Genomes Project, C. *et al.* A global reference for human genetic variation. *Nature* **526**, 68-74, doi:10.1038/nature15393 (2015).

35 Ran, F. A. *et al.* Genome engineering using the CRISPR-Cas9 system. *Nat Protoc* **8**, 2281-2308, doi:10.1038/nprot.2013.143 (2013).

36 Cong, L. *et al.* Multiplex genome engineering using CRISPR/Cas systems. *Science* **339**, 819-823, doi:10.1126/science.1231143 (2013).

37 Brinkman, E. K., Chen, T., Amendola, M. & van Steensel, B. Easy quantitative assessment of genome editing by sequence trace decomposition. *Nucleic Acids Res* **42**, e168, doi:10.1093/nar/gku936 (2014).

38 Guell, M., Yang, L. & Church, G. M. Genome editing assessment using CRISPR Genome Analyzer (CRISPR-GA). *Bioinformatics* **30**, 2968-2970, doi:10.1093/bioinformatics/btu427 (2014).

39 Park, J., Lim, K., Kim, J. S. & Bae, S. Cas-analyzer: an online tool for assessing genome editing results using NGS data. *Bioinformatics* **33**, 286-288, doi:10.1093/bioinformatics/btw561 (2017).

40 Fragouli, E. *et al.* Analysis of implantation and ongoing pregnancy rates following the transfer of mosaic diploid-aneuploid blastocysts. *Hum Genet*, doi:10.1007/s00439-017-1797-4 (2017).

41 Lou, X., Kang, M., Xenopoulos, P., Munoz-Descalzo, S. & Hadjantonakis, A. K. A rapid and efficient 2D/3D nuclear segmentation method for analysis of early mouse embryo and stem cell image data. *Stem Cell Reports* **2**, 382-397, doi:10.1016/j.stemcr.2014.01.010 (2014).

42 Vallier, L. Serum-free and feeder-free culture conditions for human embryonic stem cells. *Methods Mol Biol* **690**, 57-66, doi:10.1007/978-1-60761-962-8_3 (2011).

43 Kim, D. *et al.* TopHat2: accurate alignment of transcriptomes in the presence of insertions, deletions and gene fusions. *Genome Biol* **14**, R36, doi:10.1186/gb-2013-14-4-r36 (2013).

44 Liao, Y., Smyth, G. K. & Shi, W. featureCounts: an efficient general purpose program for assigning sequence reads to genomic features. *Bioinformatics* **30**, 923-930, doi:10.1093/bioinformatics/btt656 (2014).
45 Bacher, R. *et al.* SCnorm: robust normalization of single-cell RNA-seq data. *Nat Methods* **14**, 584-586, doi:10.1038/nmeth.4263 (2017).
46 Risso, D., Ngai, J., Speed, T. P. & Dudoit, S. Normalization of RNA-seq data using factor analysis of control genes or samples. *Nat Biotechnol* **32**, 896-902, doi:10.1038/nbt.2931 (2014).
47 Anders, S., Pyl, P. T. & Huber, W. HTSeq--a Python framework to work with high-throughput sequencing data. *Bioinformatics* **31**, 166-169, doi:10.1093/bioinformatics/btu638 (2015).
48 Love, M. I., Huber, W. & Anders, S. Moderated estimation of fold change and dispersion for RNA-seq data with DESeq2. *Genome Biol* **15**, 550, doi:10.1186/s13059-014-0550-8 (2014).
49 Mortazavi, A., Williams, B. A., McCue, K., Schaeffer, L. & Wold, B. Mapping and quantifying mammalian transcriptomes by RNA-Seq. *Nat Methods* **5**, 621-628, doi:10.1038/nmeth.1226 (2008).

Extended Data Figure 1

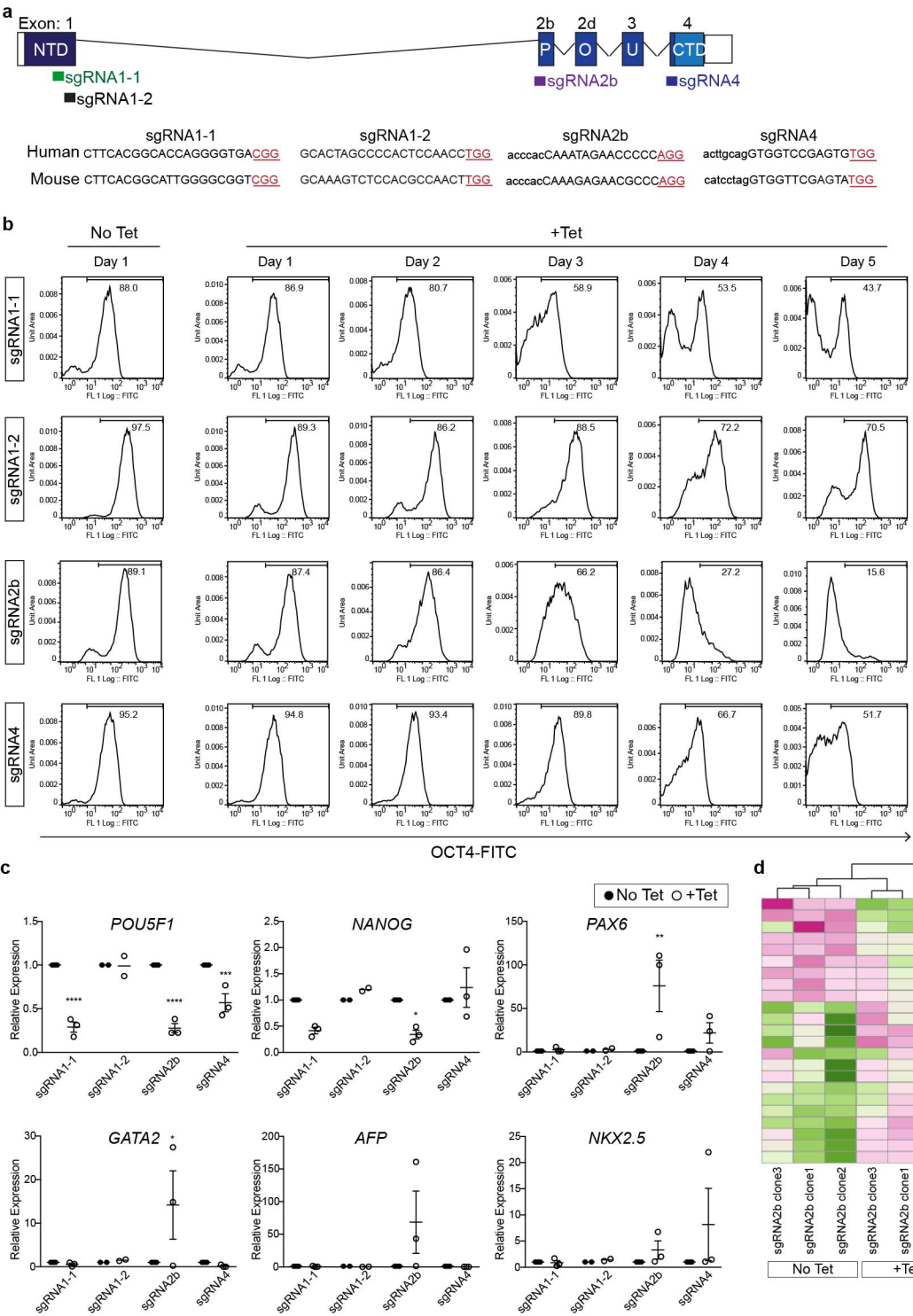

Extended Data Figure 2

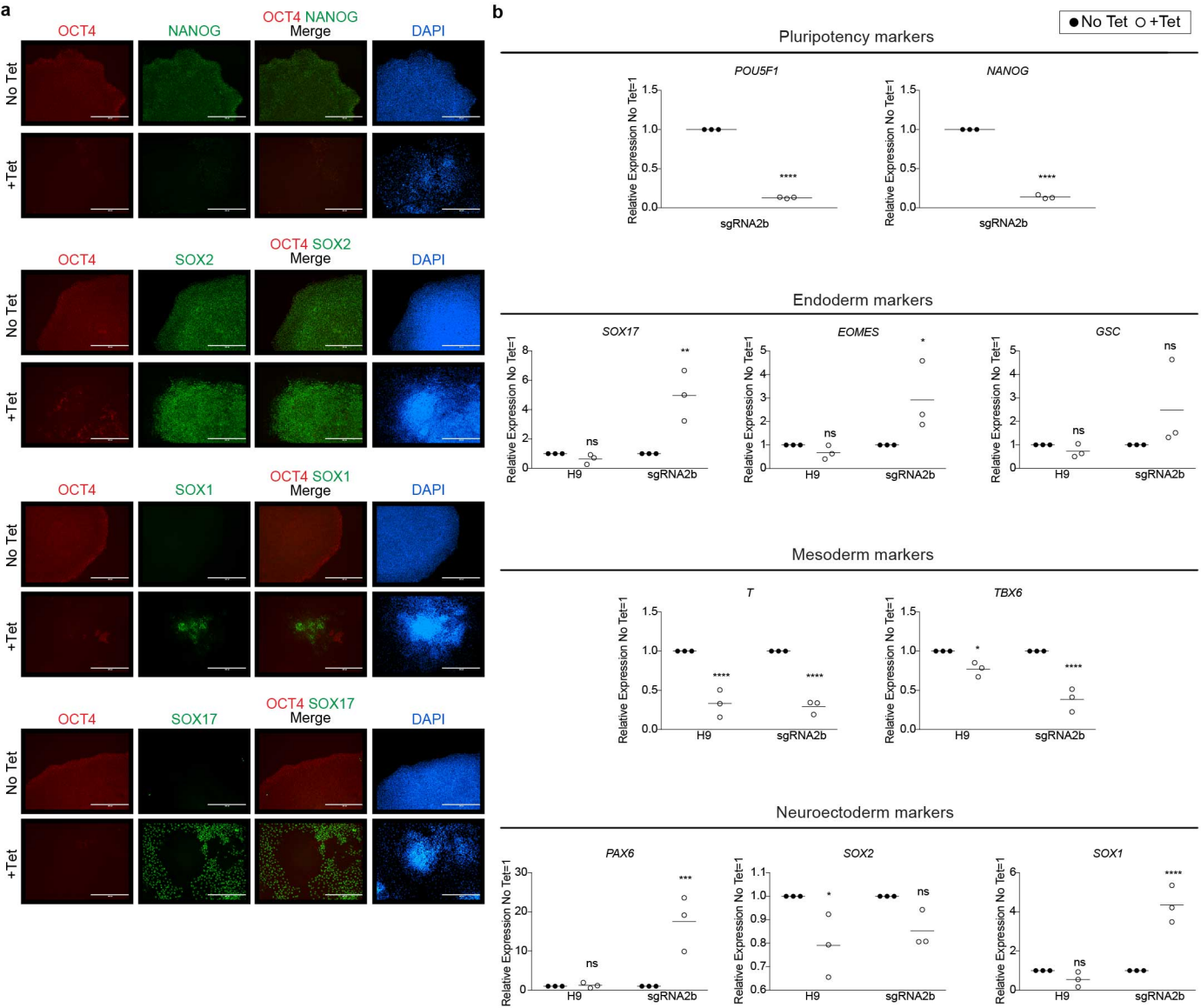

Extended Data Figure 3

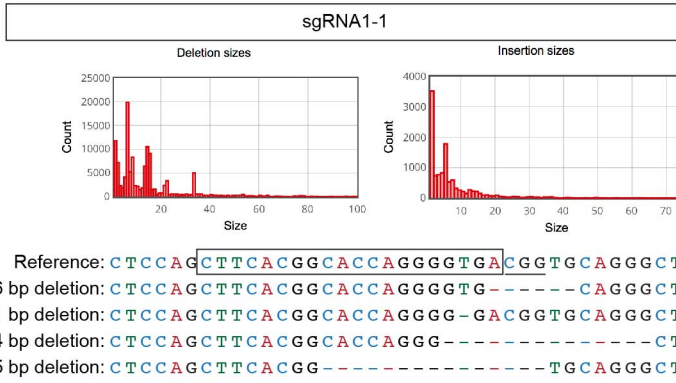

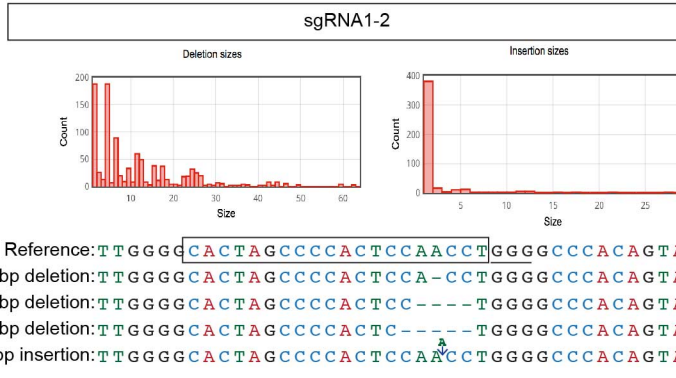

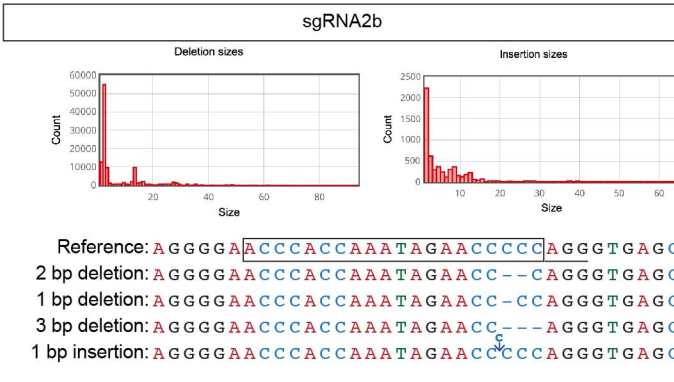

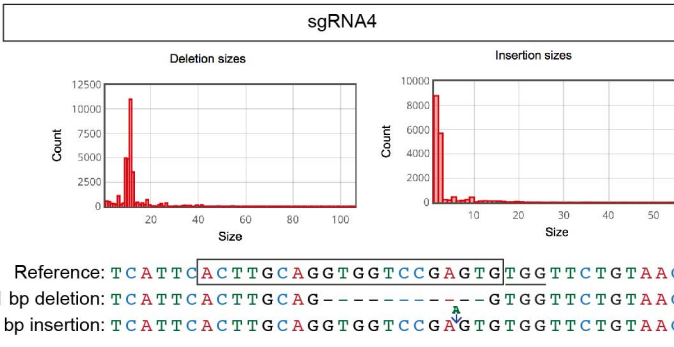

Extended Data Figure 4

a

```
ACCCACCAAATAGAACCCCCAGG  POU5F1      sgRNA2b
CCTTCCAAATAGAACCCCCAGG   POU5F1P3    ┐
CCTTCCAAATAGAACCCCCAGG   POU5F1B     │
CCTTCCAAATAGAACCCCCAGG   POU5F1P4    │ Putative off-target sites
CCTTCCAAATAGAACCCCCCAG   chr 3:+128394390 │
TATTCCAAATAGAACCCCCAGG   POU5F1P5    │
ACCCATCAAATACAACCCCCCAG  chr 19:-9072444 │
AGCCACCAGGTAGAACCCCCAAG  chr 3:+101807899 ┘
```

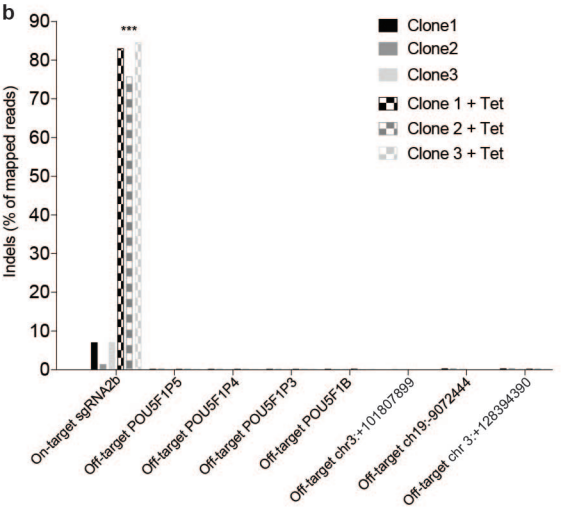

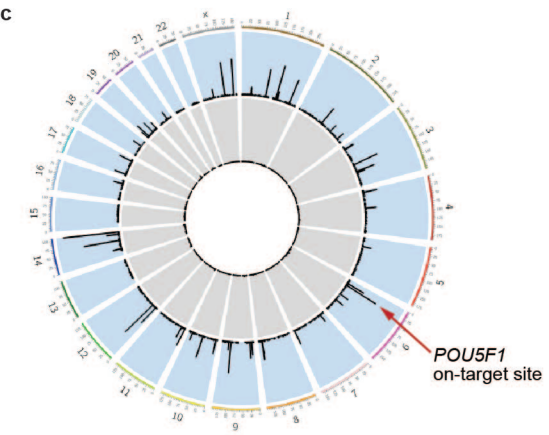

d

					Indel frequency (%) in sgRNA2b induced hESCs			
	Chr	Position	DNA cleavage Score	DNA seq at a cleavage sites	H9 control	Clone1	Clone2	Clone3
On-target	chr6	31133715	45.64	ACCCACCAAATAGAACCCCCAGG	0.18	86.64	64.05	89.49
OCT4_01	chr14	106800799	78.67	gatCACCAAATAGAAaCCCCTGG	0	0.03	0.05	0
OCT4_02	chr12	26422748	51.34	gggCcaCAtATAGAACCCCCATG	0.12	0.09	0.09	0.07
OCT4_03	chrX	139751596	47.73	ctggcatctATAGAACCCCCTAG	0.03	0.06	0.05	0.08
OCT4_04	chr14	68681659	47.6	AtaatatAAtTAGAACCCCCAAG	0.05	0.06	0.1	0.05
OCT4_06	chr1	155927429	45.19	AtCCcaaccATAGAACtCCCTGG	0	0.01	0	0.01
OCT4_07	chrX	99723295	43.65	catacCacAATAGAACCCCCAAG	0.07	0.07	0.04	0.04
OCT4_08	chr9	102171999	39.81	AgaCAaacAATAGAACCCCCATG	0.08	0.12	0.09	0.08
OCT4_09	chr1	108022179	34.37	AtttAatAtATAGAACCCCtCTG	0	0	0	0
OCT4_10	chr1	218956806	31.43	tttCcCtAAATAGAACtCCCTGG	0.45	0.6	0.45	0.53
OCT4_11	chr3	95838251	30.9	caaatCtAcATAGAACCCCCTAG	0.03	0.07	0.04	0.13
OCT4_12	chr10	69770523	25.23	tattcCCAAATAGAACCCCCAGG	0.4	0.34	0.38	0.47
OCT4_13	chr14	106825519	25.18	gatCACCAAATAGAAaCCCCTGG	0	0	0.03	0
OCT4_14	chr12	8286935	23.29	cCttcCCAAATAGAACCCCCAGG	0.59	0.51	0.54	0.77
OCT4_15	chr2	119998405	20.88	gttCtatAAATAGAACCCCCAGG	0.16	0.16	0.17	0.18
OCT4_16	chr6	21017589	20.54	tagaAgCAAATAGAACCCCtCAG	0.02	0.01	0	0.01
OCT4_17	chr8	130315051	20.33	ggtagggctATAGAACtCCCAGG	0.01	0.02	0.03	0
OCT4_18	chr3	128838949	20.16	AtaataatAATAaAACCCCtCAG	0.01	0.04	0.02	0
OCT4_19	chr11	848298	18.87	AgaCcCaccAaAGAACCCCCAGG	0.15	0.09	0.12	0.12
OCT4_20	chr1	154907795	16.34	caCacCttcATAGAACCCCCGTG	0	0	0	0
OCT4_21	chr9	16941937	15.51	gttgttattATAGAACCCCCAAG	0.13	0.09	0.11	0.07
OCT4_22	chr19	9072455	15.09	ACCCAtCAAATAcAACCCCCCAG	0.02	0	0	0.03
OCT4_23	chr7	154841143	13.49	AgaCtggcAATAGAACCCCCATG	0.09	0.1	0.08	0.07
OCT4_24	chr10	8773285	12.61	gtCCtaacAATAcAACCCCCAGG	0.14	0.12	0.16	0.11
OCT4_25	chr4	8319374	12.24	cCCacCacAATAGAACCCgCTGG	0	0	0	0
OCT4_26	chr17	72300434	11.86	cCtgcCCctATAGAACtCCCAGG	0.01	0.02	0.03	0.01
OCT4_27	chr8	128428627	10.87	cCttcCCAAATAGAACCCCCAGG	0.81	0.92	0.98	0.75
OCT4_28	chr19	35255574	10.58	ggCatatAAATAGAACCCCCTAG	0.02	0.05	0.05	0.04
OCT4_29	chr9	9376734	10.55	AagactgAAATAGAACCCCtCGG	0.01	0	0.01	0
OCT4_30	chr14	96238961	10.19	cattcaCctATAaAACCCCCTGG	0.07	0.05	0.1	0.09
OCT4_31	chr17	7412716	9.26	tttCttttcATAGAACCCCCTGG	0.06	0.05	0.08	0.04
OCT4_32	chr3	128394409	8.9	cCttcCCAAATAGAACCCCCCAG	0.02	0	0.02	0
OCT4_33	chr11	18157402	8.42	ctatAtaAtATAtAACCCCCCGG	0.01	0.01	0.01	0.01
OCT4_34	chr4	80115877	7.46	gtttAttAAATAaAACCCCCTGG	0.07	0.07	0.07	0.14
OCT4_35	chr3	16901271	6.04	caCtcCacAATAGAACCCCtTGG	0.06	0.05	0.09	0.07
OCT4_36	chr1	155403487	5.42	cCttcCCAAATAGAACCCCCAGG	0.13	0.14	0.1	0.25
OCT4_37	chr6	79233991	5.26	tgagcaagcATAGAACCCCCATG	0.06	0.15	0.12	0.08
OCT4_38	chr3	14563905	5.26	gagCtattcATAGAACCCCCGAG	0.1	0.1	0.12	0.09
OCT4_39	chr16	74025267	5.01	cCCataCccATAaAACCCCCGGG	0.04	0.1	0.11	0.09
OCT4_40	chr18	50822339	4.92	ctgtACCAAATAGAACCtCCGGG	0	0	0.01	0.01
OCT4_41	chr6	110709371	4.78	cttagaatAATAaAACCCCCAGG	0.14	0.16	0.15	0.17
OCT4_42	chr20	41865179	4.42	AgggtaatAATAGAACCCCtCGG	0	0	0.01	0
OCT4_43	chr14	30269627	4.1	AaCCcaCcAATAaAACCCCaGGG	0.07	0.04	0.08	0.06
OCT4_44	chr5	42242481	3.98	AaaCcaCcAATtaAACCCCCAGG	0.12	0.14	0.15	0.19
OCT4_45	chrX	49584622	3.85	cCCtgCtctATAGAACCCCtGGG	0	0	0	0
OCT4_46	chr1	162161716	3.68	AgCagtagAATAGAACCCCCTAG	0.05	0.06	0.03	0.07
OCT4_47	chr7	18632224	3.49	ACtCtttAAATAGAACtCCCAGG	0.06	0.04	0.03	0.04
OCT4_48	chr10	119000954	3.43	AgaCcCaAccTAGAACCCCCAGG	No PCR			
OCT4_49	chr2	173218580	3.31	tCtaAtacAATAcAACCCCCAGG	0.14	0.19	0.14	0.16
OCT4_50	chr19	58212321	3.31	cCCataCAtATAGAACCCCCAAG	0.04	0.06	0.09	0.07
OCT4_51	chr3	134489132	3.21	AtgtttttAATAGAACCCCCAGG	0.14	0.14	0.2	0.12
OCT4_52	chr2	220000671	3.14	AagtAagAtATAcAACCCCCTGG	0.08	0.07	0.07	0.08
OCT4_53	chr19	1638064	3.12	cttCAttccATAGAACCCCCAGG	0.25	0.29	0.21	0.22
OCT4_54	chr9	112131872	2.81	AaaaAtacAATAGAACtCCCTGG	0.02	0.01	0.01	0.01
OCT4_55	chr1	42277717	2.52	caatggtAtAaAGAACCCCCAAG	0.08	0.05	0.06	0.06

f

				Indel frequency (%) in sgRNA2b induced hESCs			
	Chr	Position	DNA seq at a cleavage sites	H9 control	Clone1	Clone2	Clone3
OCT4_m3_01	chr2	1420732	ACCCACCAAgcAGgACCCCCCGG	0.02	0	0	0
OCT4_m3_02	chr11	29005836	ACCCgCCAAtTAGAACtCCCTGG	0	0.02	0	0
OCT4_m3_03	chr19	33491466	ACCCACCAcAcAGAACCtCCTGG	0	0	0	0
OCT4_m3_04	chr1	34088933	ACCCtCCAAATtGAAgCCCCTGG	0.03	0.07	0.02	0.04
OCT4_m3_05	chr3	41725076	ACCCAaCAAATAGAAgaCCCAGG	3.4	3.46	3.71	3.56
OCT4_m3_06	chr8	53679039	ACtCACCAAgTAGAACtCCCTGG	0	0	0	0
OCT4_m3_07	chr14	70670673	ACCCACCAAcTAGAACtCtCAGG	0	0	0	0
OCT4_m3_08	chr3	71533567	ACCCACCAAATAGtgCCaCCTGG	0.01	0.02	0	0.01
OCT4_m3_09	chr6	77294186	ACCCcCCAAAgAGAACaCCCAGG	0.01	0.03	0.03	0
OCT4_m3_10	chrX	122754088	ACCCAgCAAAgAGAAaCCCCAGG	0.08	0.09	0.15	0.06
OCT4_m3_11	chr12	125649468	ACCCACCAAcTAcAtCCCCCAGG	0.09	0.17	0.12	0.08
OCT4_m3_12	chr5	178189342	ACCCACCAAcTAcAtCCCCCAGG	0.11	0.15	0.09	0.11

Extended Data Figure 5

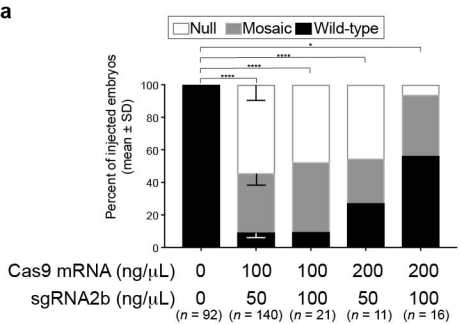

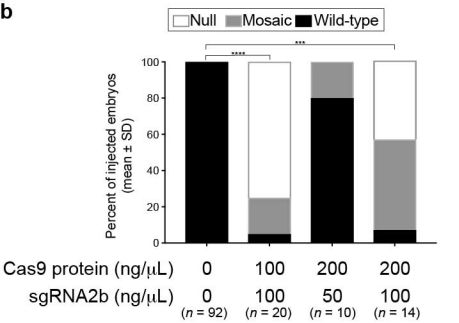

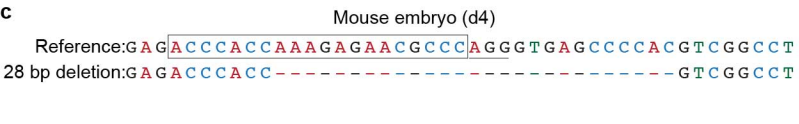

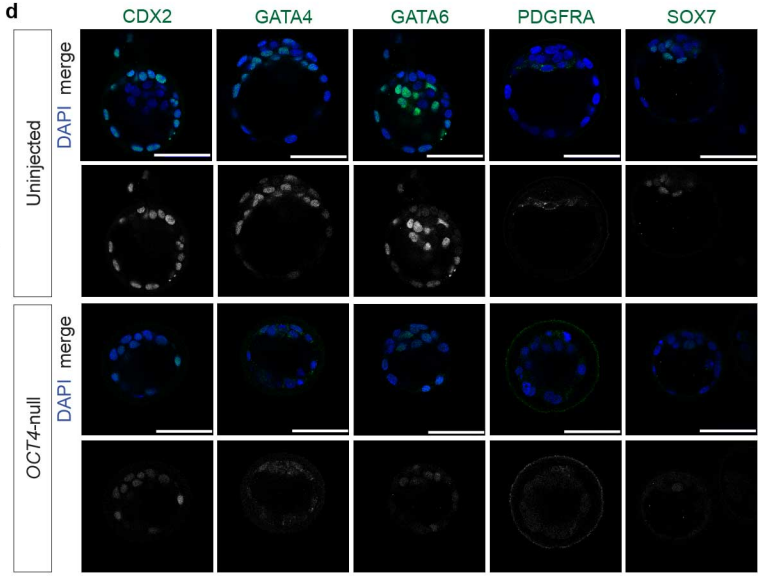

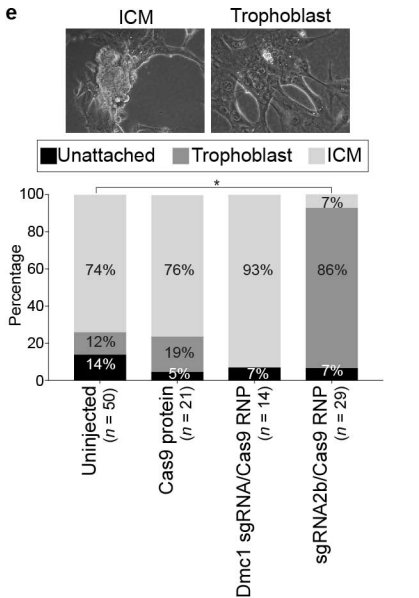

Extended Data Figure 6

a

Karyotype analysis of Cas9 control or sgRNA2b/Cas9 ribonucleoprotein complex microinjected embryos

	Embryo ID	Stage	Sample collected	Karyotype (chromosome gain/loss)
sgRNA2b/Cas9 ribonucleoprotein complex injected	**C1**	Cleavage	3 cell arrested embryo	46 XX (-chr15, +chr18)
	C2	Blastocyst	3-5 cells from the TE	46 XY
	C3	Cleavage	1 cell from 8-cell arrested embryo	46 XO (-Xchr)
	C4	Cleavage	1 cell from -cell arrested embryo	46 XY
	C8 (sample1)	Blastocyst	3-5 cells from the TE	46 XY
	C8 (sample2)	Blastocyst	3-5 cells from the TE	46 XY
	C8 (sample3)	Blastocyst	3-5 cells from the TE	46 XY
	C9	Blastocyst	2-3 cells from the TE	43 XXX (-chr7, +chr11, -chr12, -chr14, -chr18, +Xchr)
	C10	Cleavage	1 cell from 8 cell arrested embryo	46 XX (-chr7, +chr14)
	C12 (sample1)	Blastocyst	3-5 cells from the TE	46 XX
	C12 (sample2)	Blastocyst	3-5 cells from the TE	46 XX
	C14	Cleavage	1 cell from 2-cell arrested embryo	47 XY (+chr16)
	C15	Cleavage	1 cell from 6-cell arrested embryo	46 XX (+chr1, +chr2, -chr12, -chr20)
	C16 (sample1)	Blastocyst	3-5 cells from the TE	45 XY (-chr16)
	C16 (sample2)	Blastocyst	3-5 cells from the TE	45 XY (-chr16)
Cas9 protein injected	**5K**	Blastocyst	3-5 cells from the TE	46 XX
	7K	Blastocyst	3-5 cells from the TE	45 XX (-chr14)
	8K	Blastocyst	3-5 cells from the TE	47 XX (-chr14, +chr15, +chr18)
	1K	Blastocyst	3-5 cells from the TE	46 XY
	2K	Blastocyst	3-5 cells from the TE	46 XY
	3K	Blastocyst	3-5 cells from the TE	46 XX
	4K	Blastocyst	3-5 cells from the TE	45 XX (-chr21)

b

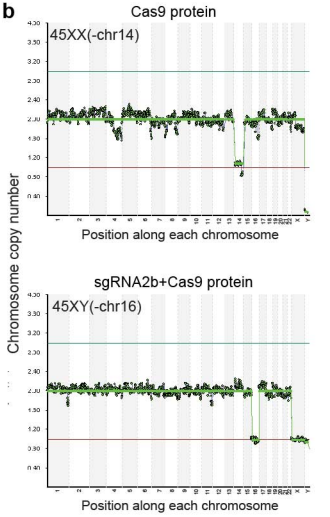

c

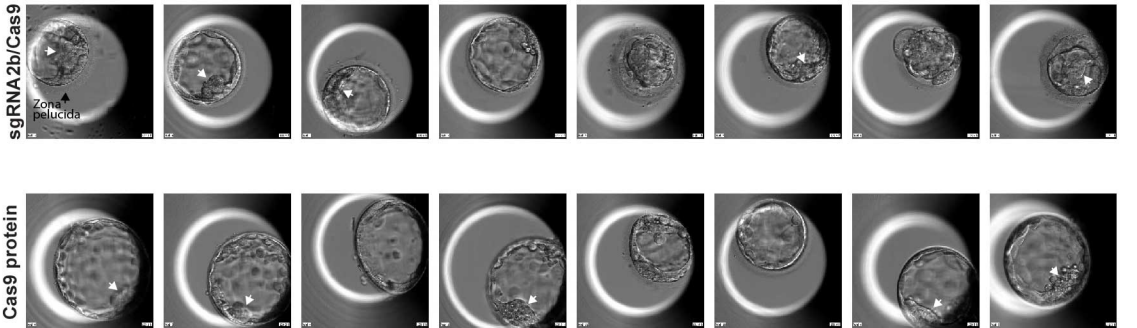

Extended Data Figure 7

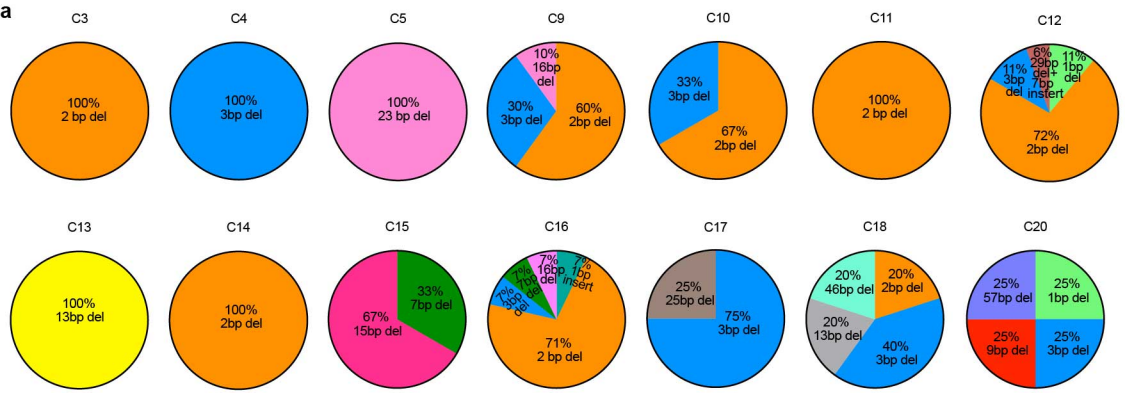

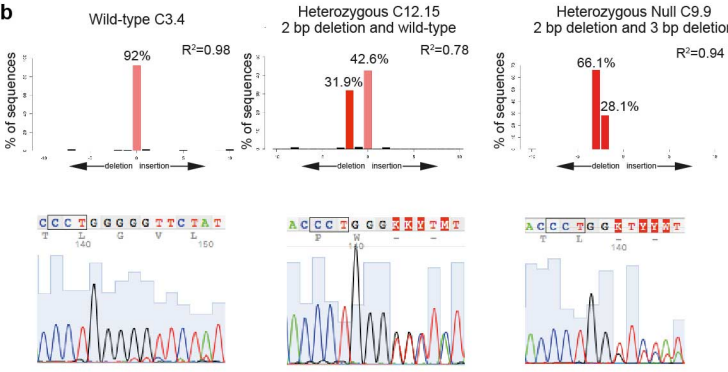

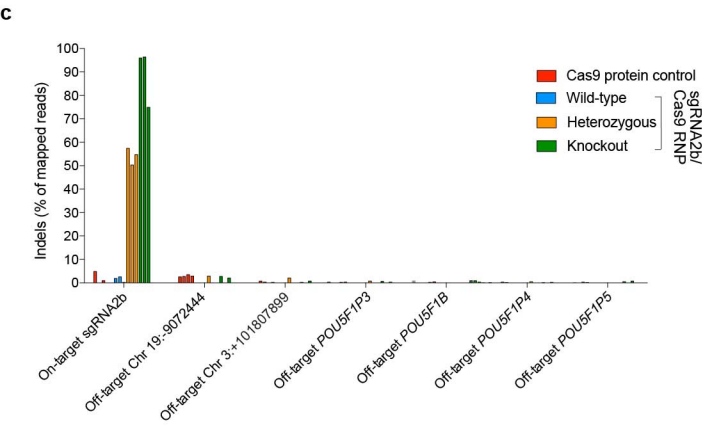

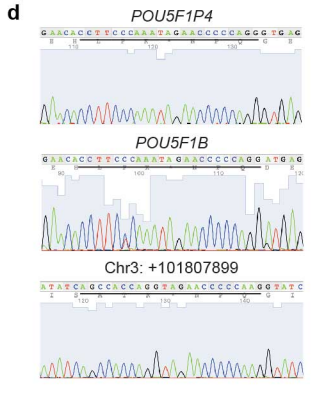

Extended Data Figure 8

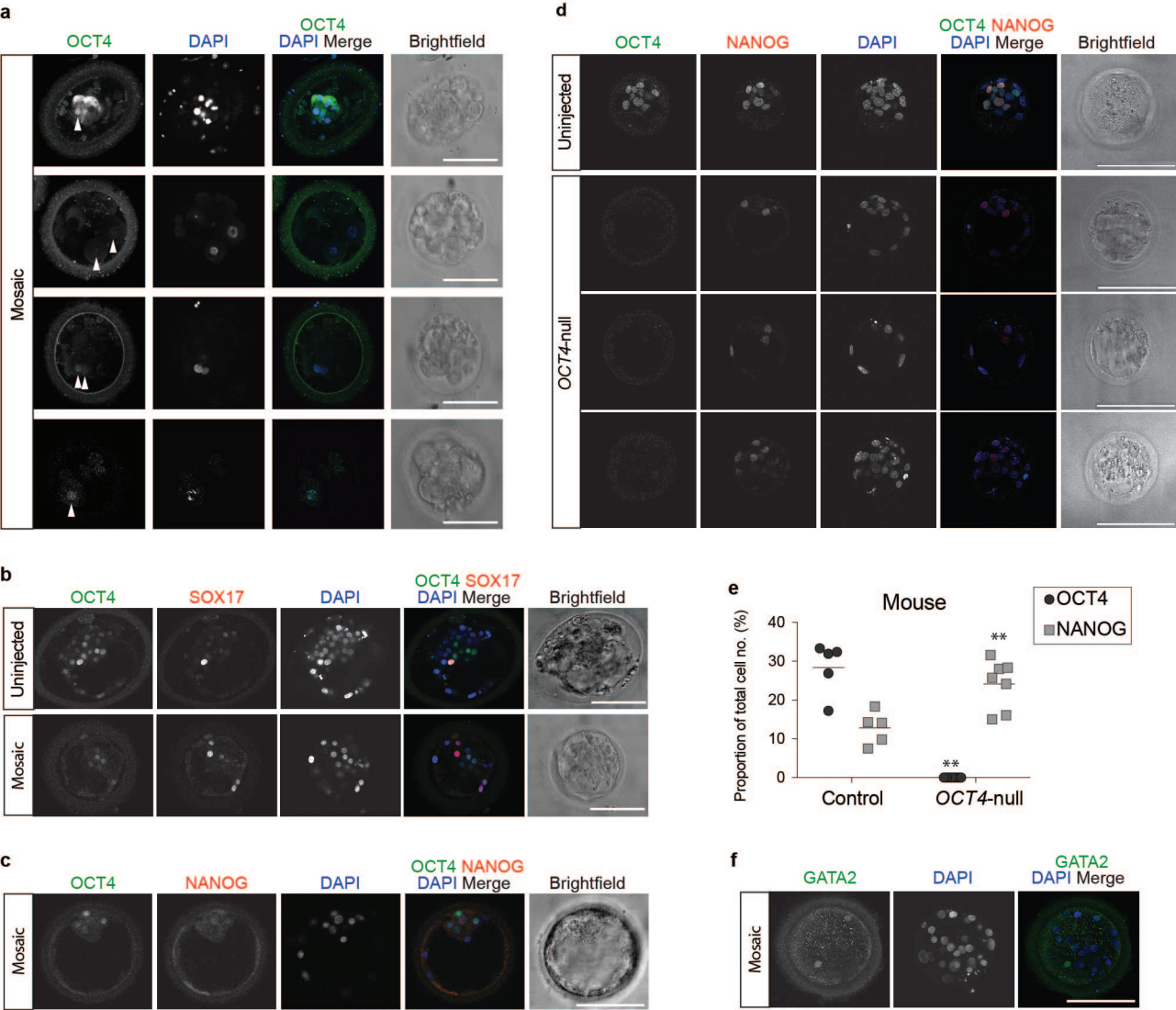

Extended Data Figure 9

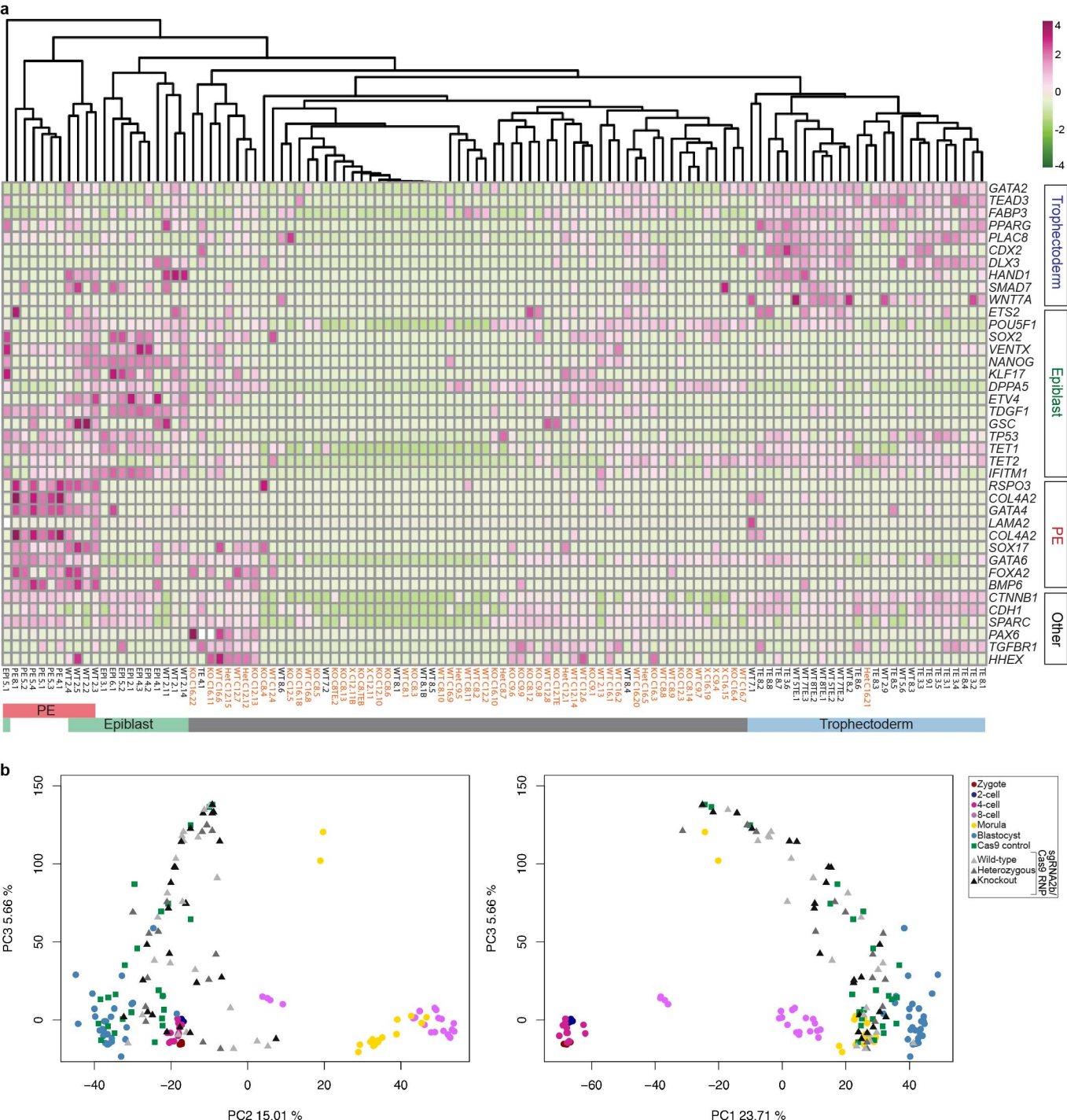

Extended Data Figure 10

a

Engineering tetracycline-inducible hESCs targeting the endogenous *AAVS1* locus

sgRNA	Top oligo for cloning	Bottom oligo for cloning
sgRNA1-1	TCCCGCTTCACGGCACCAGGGGTGA	AAACTCACCCCTGGTGCCGTGAAGC
sgRNA1-2	TCCCGCACTAGCCCCACTCCAACC	AAACGGTTGGAGTGGGGCTAGTGC
sgRNA2b	TCCCACCCACCAAATAGAACCCCC	AAACGGGGGTTCTATTTGGTGGGT
sgRNA4	TCCCACTTGCAGGTGGTCCGAGTG	AAACCACTCGGACCACCTGCAAGT

***In vitro* transcription of human sgRNAs**

sgRNA	Forward	Reverse	T7 Guide Primer
sgRNA1-1	CACCGCTTCACGGCACCAGGGGTGA	AAACTCACCCCTGGTGCCGTGAAGC	TTAATACGACTCACTATAGGGGGCGTTCTCTTTGGTGGGT
sgRNA2b	CACCGACCCACCAAATAGAACCCCC	AAACGGGGGTTCTATTTGGTGGGTC	TTAATACGACTCACTATAGGACCCACCAAATAGAACCCCC
sgRNA4	CACCGACTTGCAGGTGGTCCGAGTG	AAACCACTCGGACCACCTGCAAGTC	TTAATACGACTCACTATAGGACTTGCAGGTGGTCCGAGTG

***In vitro* transcription of mouse sgRNAs**

sgRNA	*Forward*	*Reverse*	*T7 Guide Primer*
sgRNA1-1	CACCGCTTCACGGCATTGGGGCGGT	AAACACCGCCCCAATGCCGTGAAGC	TTAATACGACTCACTATAGGCTTCACGGCATTGGGGCGGT
sgRNA1-2	CACCGGCAAAGTCTCCACGCCAACT	AAACAGTTGGCGTGGAGACTTTGCC	TTAATACGACTCACTATAGGGCAAAGTCTCCACGCCAACT
sgRNA2b	CACCGACCCACCAAAGAGAACGCCC	AAACGGGCGTTCTCTTTGGTGGGTC	TTAATACGACTCACTATAGGACCCACCAAAGAGAACGCCC
sgRNA4	CACCGCATCCTAGGTGGTTCGAGTA	AAACTACTCGAACCACCTAGGATGC	TTAATACGACTCACTATAGGCATCCTAGGTGGTTCGAGTA
Dmc1 sgRNA	CACCGTAGGAATCTGTACCATTAA	AAACTTAATGGTACAGATTCCTAC	TTAATACGACTCACTATAGGGTAGGAATCTGTACCATTA

Universal Reverse Primer for IVT AAAAGCACCGACTCGGTGCC

MiSeq and/or Sanger sequencing analysis of human cells

Site	Forward oligo	Reverse oligo
sgRNA1-1 on-target site	CTGTGGGCCCCAGGTT	ATCAGGCTGCCCTGTCAT
sgRNA1-2 on-target site	TGGAGGTGATGGGCCAG	ACCAGGGGTGACGGTG
sgRNA2b on-target site (used primarily)	AGGGGAGATTGATAACTGGTGT	ACTAGGTTCAGGGATACTCCTTAG
sgRNA2b on-target site 1000bp	CGCCCAGCAAAGAACTTCTA	GAGAACCACTGCACCAAAGA
sgRNA2b on-target site 800bp	TGCATGAGTCAGTGAACAGG	GAGAACCACTGCACCAAAGA*
sgRNA2b on-target site 140bp	CATGGGTGAGGGTAGTCTGC	TGGGATATACACAGGCCGAT
sgRNA2b upstream of on-target site	CTTCAGGAGCTTGGCAAATTG	AGGGGAGATTGATAACTGGTGT
sgRNA2b downstream of on-target site	CAGATGGTCGTTTGGCTGAA	TCTGGGAAGAGGTGGTAAGC
sgRNA4 on-target site	TGTCCTCCTCTAACTGCTCT	CAGAGGAAAGGACACTGGTC
NR_036440 putative off-target site	CCTGCACGAGGGTTTCTG	AAGGAGTCCCAGGACATCAA
NM_001159542 putative off-target site	AACCCGGAGAAGTCCCAG	TGTTGTCAGCTTCCTCCAC
NR_034180 putative off-target site	GCAGGAGTCCCAGAACATC	GGGTTTCTGCTTTGCATGTC
NR_131184 putative off-target site	CCAGTCCCAGGACATCTCAA	ACTTCTGCAGCAAGGGC
chr3:+101807899 putative off-target site	TATGTGGGCTGGCATTCATAC	TTTTCACCATGGAGCATTGAGTA
chr3:+128394390 putative off-target site	ACGGGGTTTCTCCATGTTAC	CTCTTCATTGTTGGCTGCTT
chr19:-9072444 putative off-target site	CCGAGGTATCCAGGACAGAT	ATCCACAGAGGGAGGACTTG

MiSeq analysis of mouse cells

Site	Forward oligo	Reverse oligo
sgRNA2b on-target site	GAACAGTTTGCCAAGCTGCT	CCCCACCTCTGACAGTTCAA
Dmc1 on-target site	GATGGACACGAAGCTCATGAC	CAATAAGCTTGTTGGCTGCCTC

qRT-PCR

Gene	Forward oligo	Reverse oligo
POU5F1	AGTGAGAGGCAACCTGGAGA	ACACTCGGACCACATCCTTC
GAPDH	GATGACATCAAGAAGGTGGTG	GTCTACATGGCAACTGTGAGG
NANOG	CATGAGTGTGGATCCAGCTTG	CCTGAATAAGCAGATCCATGG
SOX2	TGGACAGTTACGCGCACAT	CGAGTAGGACATGCTGTAGGT
GATA6	TCCACTCGTGTCTGCTTTTG	TCCTAGTCCTGGCTTCTGGA
SOX17	CGCACGGAATTTGAACAGTA	GGATCAGGGACCTGTCACAC
AFP	ACCATGAAGTGGGTGGAATC	TGGTAGCCAGGTCAGCTAAA
PAX6	TCTAATCGAAGGGCCAAATG	TGTGAGGGCTGTGTCTGTTC
PAX6	CTTTGCTTGGGAAATCCGAG	AGCCAGGTTGCGAAGAACTC
NESTIN	GAAACAGCCATAGAGGGCAAA	TGGTTTTCCAGAGTCTTCAGTGA
ISL1	GTGCAAGGACAAGAAGCGAA	TATGTCACTCTGCAAGGCGA
NKX2.5	CCTCAACAGCTCCCTGACTC	AGGCTGCAGGATCACTCATT
KRT18	CTGCTGCACCTTGAGTCAGA	TGGTGGTCTTTTGGATGGTT
CDX2	GGAACCTGTGCGAGTGGAT	TCGATATTTGTCTTTCGTCCT
GATA2	CAGACGAAGGCAACCATTTT	CAGAGGAGAAGAGGGTGCAG
GSC	GAGGAGAAAGTGGAGGTCTGGTT	CTCTGATGAGGACCGCTTCTG
SOX1	FW+ REV: Quantitec primers (Qiagen): QT00215299	
TBX6	AAGTACCAACCCCGCATACA	TAGGCTGTCACGGAGATGAA
PBGD	GGAGCCATGTCTGGTAACGG	CCACGCGAATCACTCTCATCT
RPLP0	GGCGTCCTCGTGGAAGTGAC	GCCTTGCGCATCATGGTGTT

b

Antibody	Product Number	Source	Dilution
Anti NANOG	REC-RCAB0001P	2B Scientific	1:250
Anti NANOG	AF1997	R&D	1:100
Anti GATA4	SC-25310	Santa Cruz	1:250
Anti SOX7	AF2766	R&D	1:250
Anti PDGFRA	14-1401-82	e-Boiscience labs	1:250
Anti CDX2	MU392A-UC	Biogenex	1:250
Anti GATA6	AF1700	R&D	1:250
Anti OCT4	SC-5279	Santa Cruz	1:250
Anti SOX17	AF1924	R&D	1:500
Anti SOX1	AF3369	R&D	1:1000
Anti PAX6	PAX6	DSHB	1:10
Anti ZO-1	61-7300	Thermo Fisher	1:250
Anti GATA2	sc-9008	Santa Cruz	1:250

Figure 1

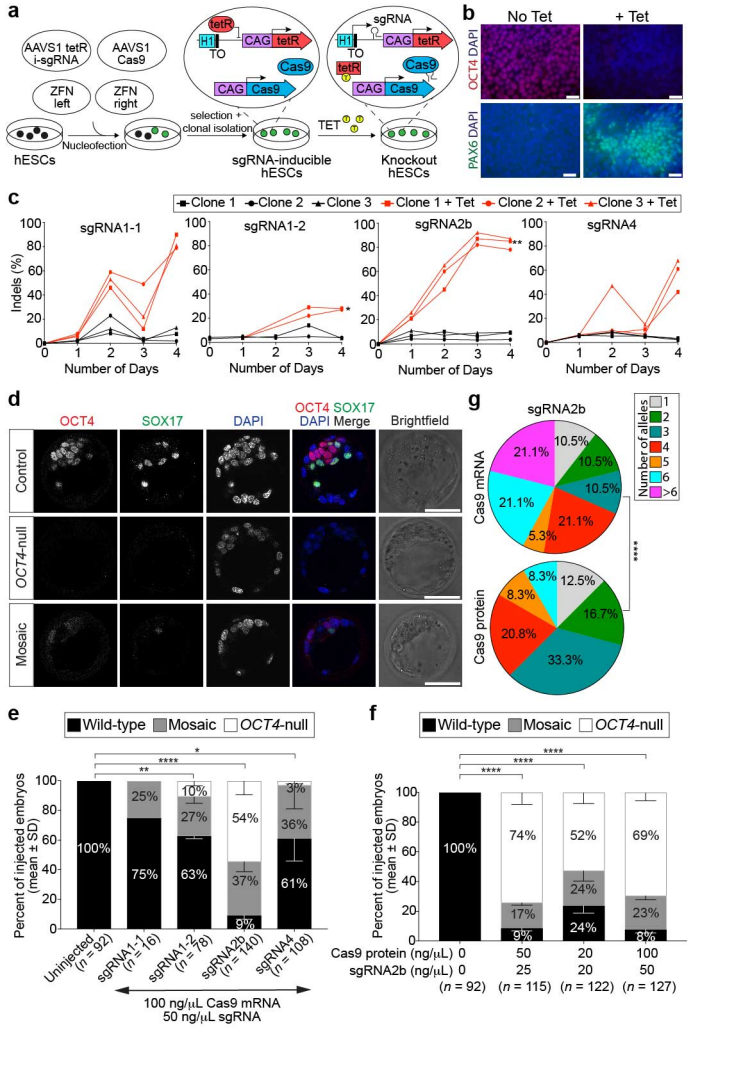
a
AAVS1 tetR i-sgRNA
AAVS1 Cas9
ZFN left
ZFN right
Nucleofection
hESCs
selection + clonal isolation
sgRNA-inducible hESCs
TET
Knockout hESCs
sgRNA
b
No Tet
+ Tet
OCT4 DAPI
PAX6 DAPI
c
Clone 1
Clone 2
Clone 3
Clone 1 + Tet
Clone 2 + Tet
Clone 3 + Tet
sgRNA1-1
sgRNA1-2
sgRNA2b
sgRNA4
Indels (%)
Number of Days
d
OCT4
SOX17
DAPI
OCT4 SOX17 DAPI Merge
Brightfield
Control
OCT4-null
Mosaic
g
sgRNA2b
Cas9 mRNA
Cas9 protein
Number of alleles
1
2
3
4
5
6
>6
10.5%
10.5%
10.5%
21.1%
21.1%
5.3%
8.3%
12.5%
16.7%
20.8%
33.3%
e
Wild-type
Mosaic
OCT4-null
Percent of injected embryos (mean ± SD)
100%
25%
75%
10%
27%
63%
54%
37%
9%
3%
36%
61%
Uninjected (n = 92)
sgRNA1-1 (n = 16)
sgRNA1-2 (n = 78)
sgRNA2b (n = 140)
sgRNA4 (n = 108)
100 ng/μL Cas9 mRNA
50 ng/μL sgRNA
f
Wild-type
Mosaic
OCT4-null
Percent of injected embryos (mean ± SD)
100%
74%
17%
9%
52%
24%
24%
69%
23%
8%
Cas9 protein (ng/μL) 0 50 20 100
sgRNA2b (ng/μL) 0 25 20 50
(n = 92) (n = 115) (n = 122) (n = 127)

Figure 2

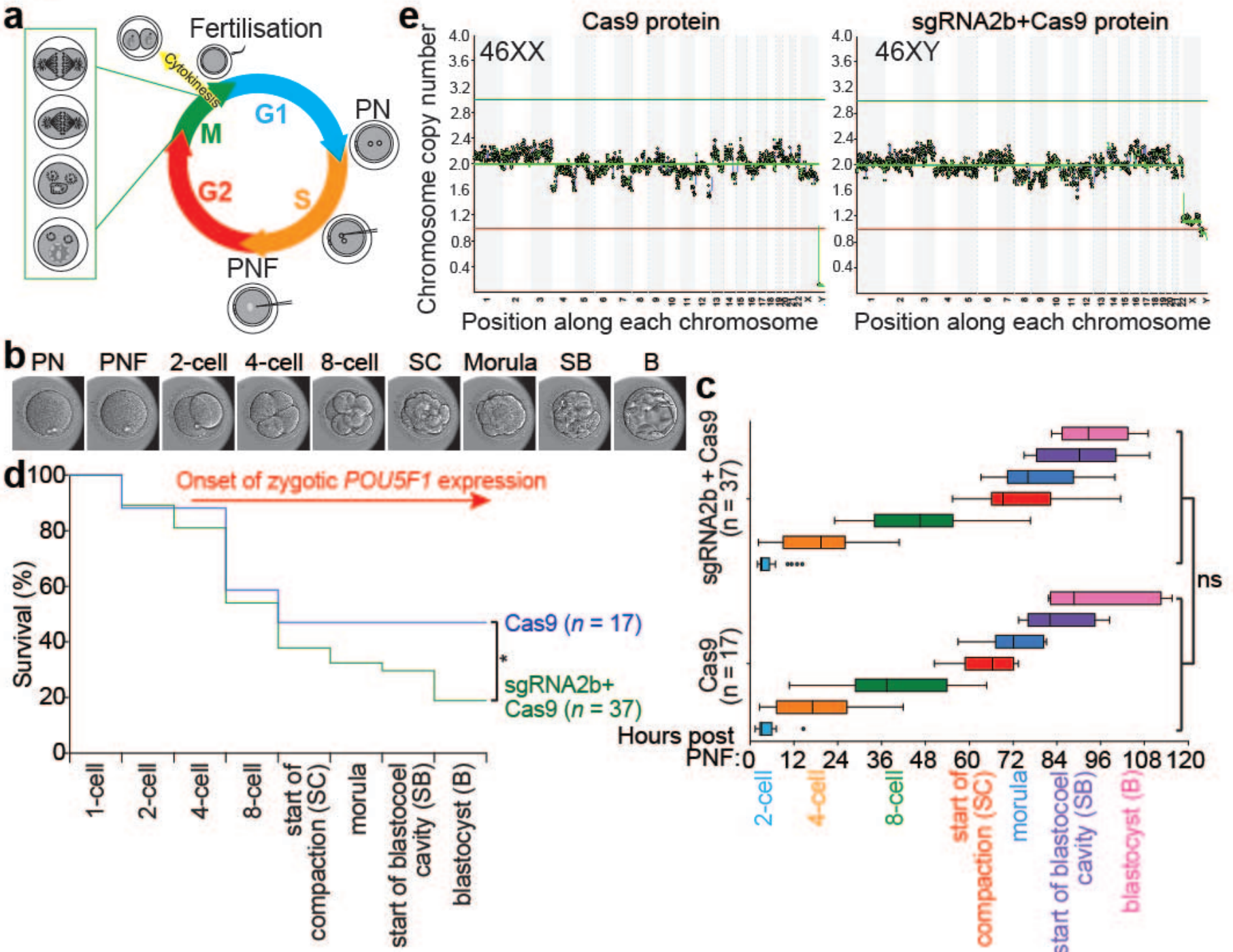
a
Fertilisation
Cytokinesis
G1
PN
M
G2
S
PNF
e
Cas9 protein
sgRNA2b+Cas9 protein
46XX
46XY
Chromosome copy number
Position along each chromosome
b
PN
PNF
2-cell
4-cell
8-cell
SC
Morula
SB
B
c
sgRNA2b + Cas9 (n = 37)
Cas9 (n = 17)
ns
Hours post PNF:
0 12 24 36 48 60 72 84 96 108 120
2-cell
4-cell
8-cell
start of compaction (SC)
morula
start of blastocoel cavity (SB)
blastocyst (B)
d
Onset of zygotic POU5F1 expression
Survival (%)
Cas9 (n = 17)
sgRNA2b+ Cas9 (n = 37)
*
1-cell
2-cell
4-cell
8-cell
start of compaction (SC)
morula
start of blastocoel cavity (SB)
blastocyst (B)

Figure 3

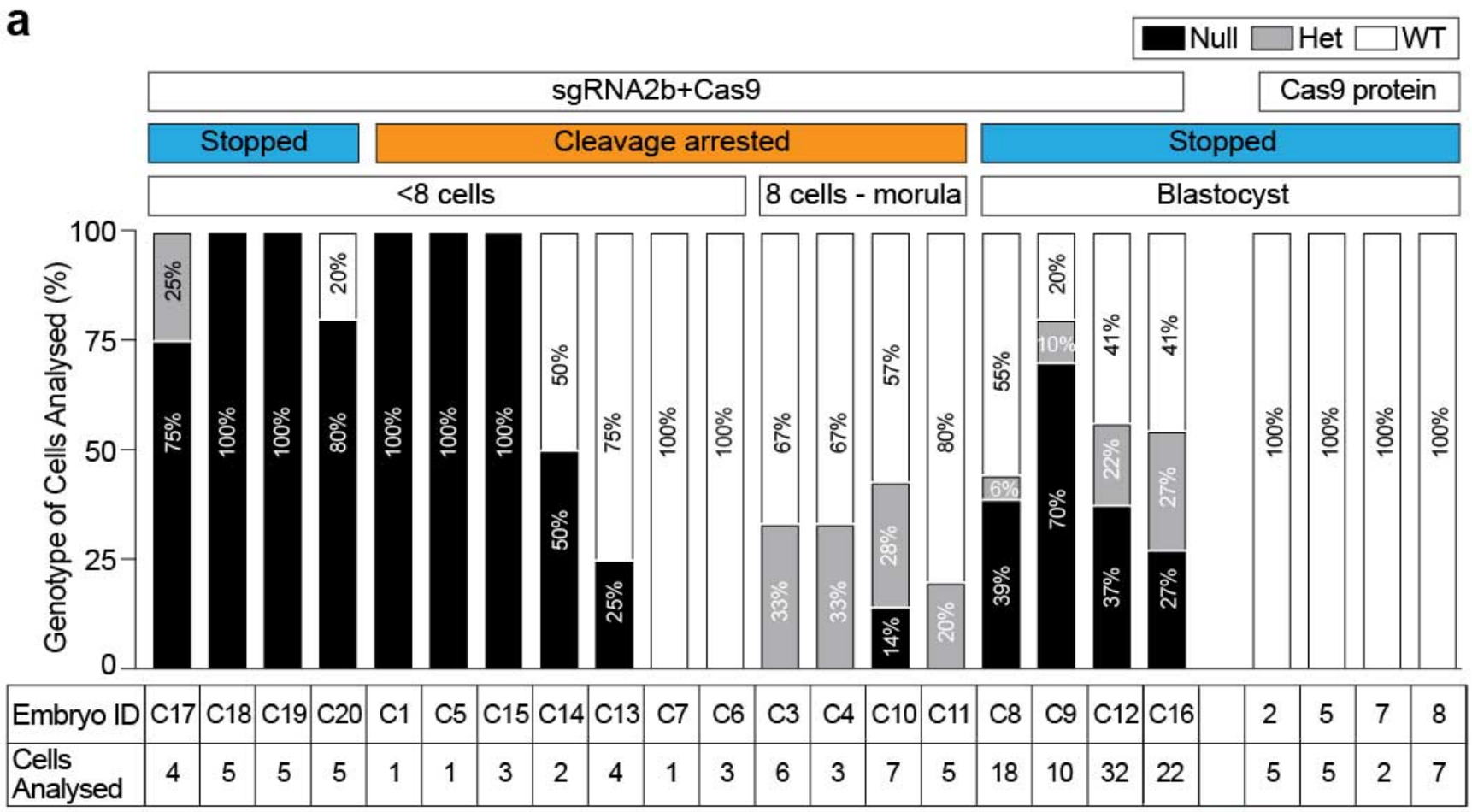
a
Null
Het
WT
sgRNA2b+Cas9
Cas9 protein
Stopped
Cleavage arrested
Stopped
<8 cells
8 cells - morula
Blastocyst
Genotype of Cells Analysed (%)
100
75
50
25
0
25%
75%
100%
20%
80%
50%
50%
75%
25%
67%
33%
57%
28%
14%
80%
20%
55%
6%
39%
20%
10%
70%
41%
22%
37%
41%
27%
27%
Embryo ID
C17
C18
C19
C20
C1
C5
C15
C14
C13
C7
C6
C3
C4
C10
C11
C8
C9
C12
C16
2
5
7
8
Cells Analysed
4
5
5
5
1
1
3
2
4
1
3
6
3
7
5
18
10
32
22
5
5
2
7

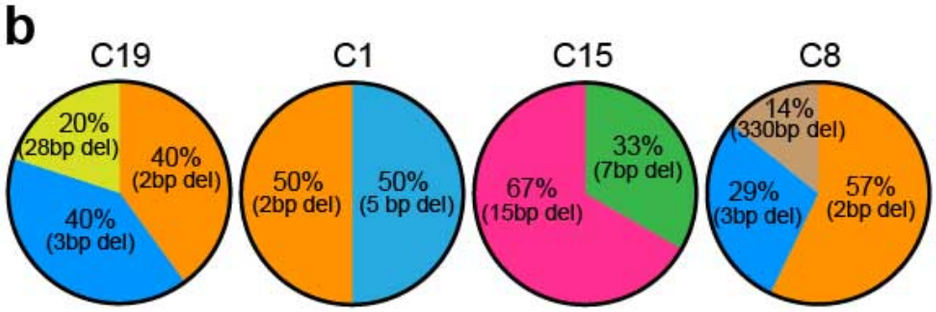
b
C19
20% (28bp del)
40% (2bp del)
40% (3bp del)
C1
50% (2bp del)
50% (5 bp del)
C15
33% (7bp del)
67% (15bp del)
C8
14% (330bp del)
29% (3bp del)
57% (2bp del)

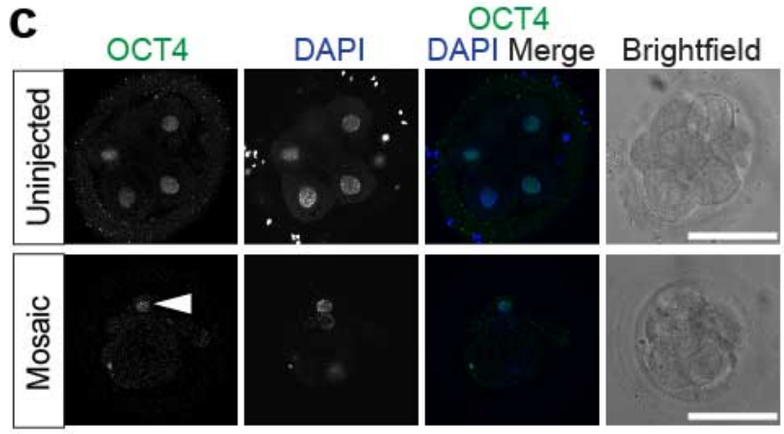
c
OCT4
DAPI
OCT4 DAPI Merge
Brightfield
Uninjected
Mosaic

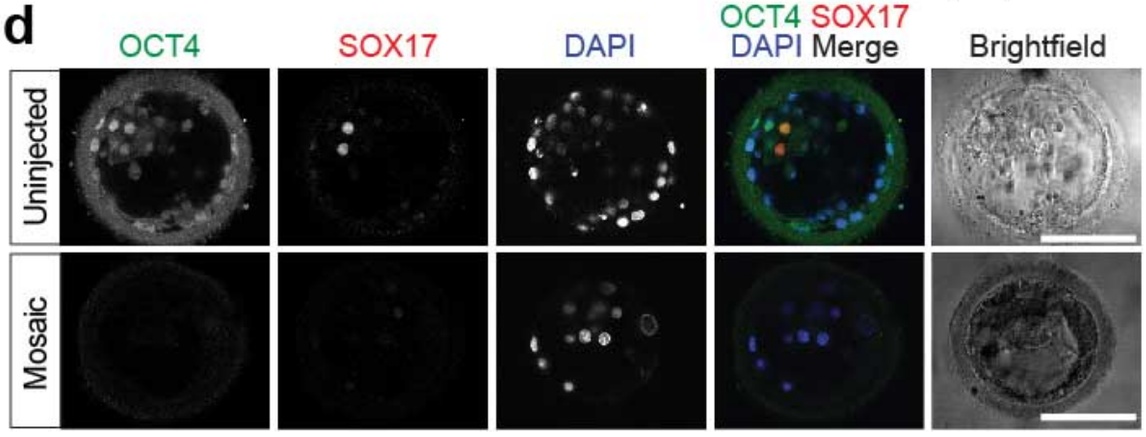
d
OCT4
SOX17
DAPI
OCT4 SOX17 DAPI Merge
Brightfield
Uninjected
Mosaic

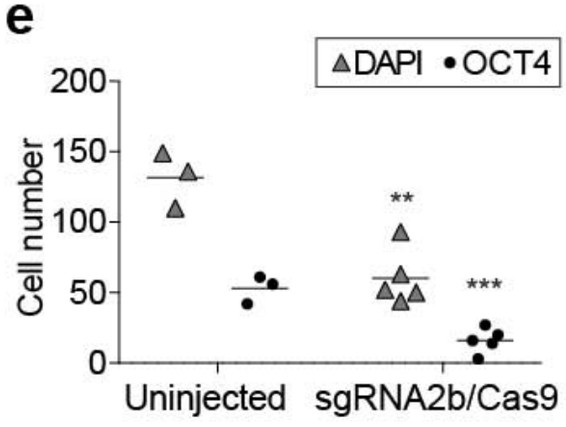
e
DAPI
OCT4
Cell number
200
150
100
50
0
**
***
Uninjected
sgRNA2b/Cas9

Figure 4

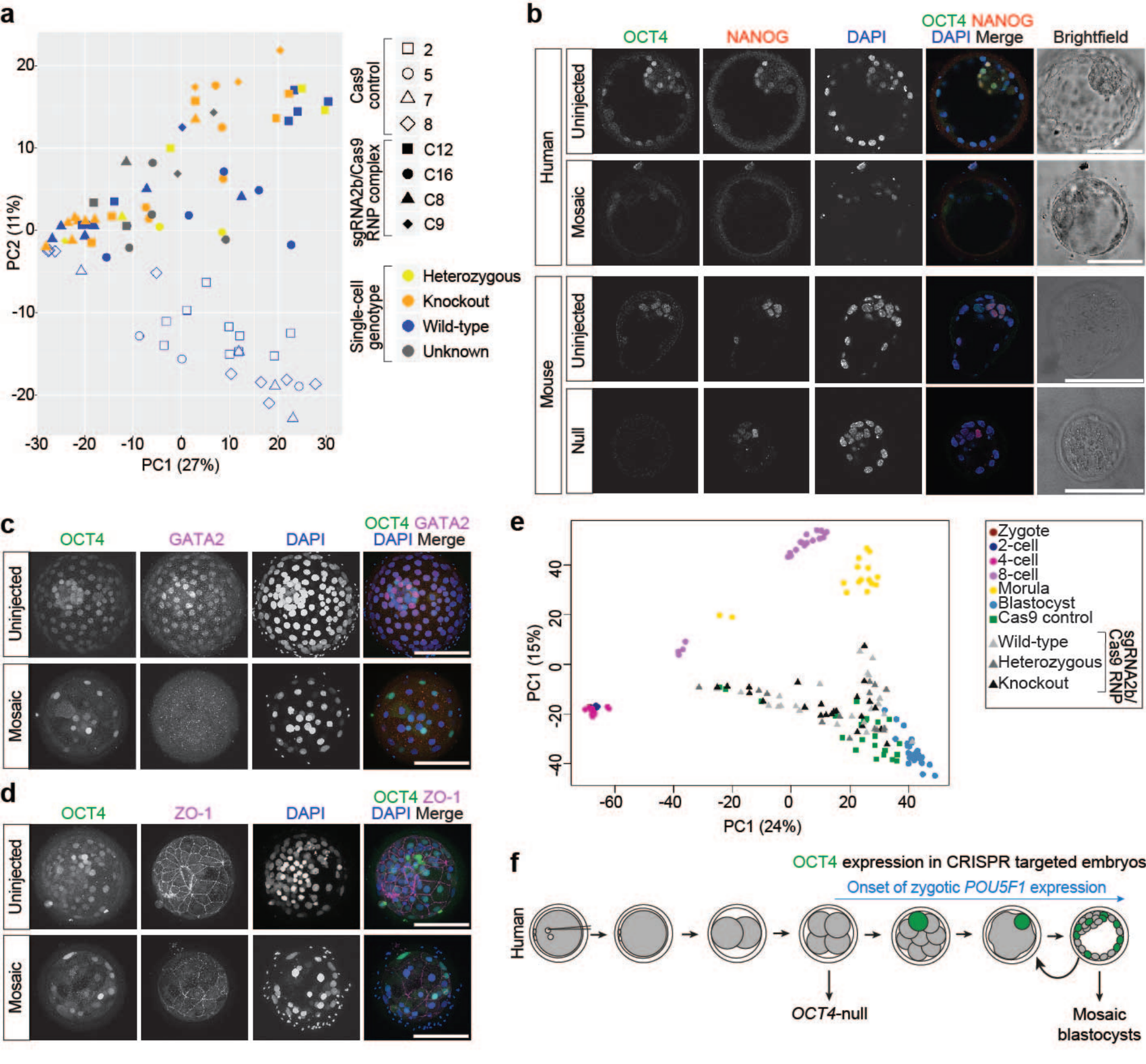
a
PC2 (11%)
PC1 (27%)
Cas9 control
2
5
7
8
sgRNA2b/Cas9 RNP complex
C12
C16
C8
C9
Single-cell genotype
Heterozygous
Knockout
Wild-type
Unknown
b
OCT4
NANOG
DAPI
OCT4 NANOG DAPI Merge
Brightfield
Human
Mouse
Uninjected
Mosaic
Null
c
OCT4
GATA2
DAPI
OCT4 GATA2 DAPI Merge
Uninjected
Mosaic
d
OCT4
ZO-1
DAPI
OCT4 ZO-1 DAPI Merge
Uninjected
Mosaic
e
PC1 (15%)
PC1 (24%)
Zygote
2-cell
4-cell
8-cell
Morula
Blastocyst
Cas9 control
Wild-type
Heterozygous
Knockout
sgRNA2b/Cas9 RNP
f
OCT4 expression in CRISPR targeted embryos
Onset of zygotic POU5F1 expression
Human
OCT4-null
Mosaic blastocysts